



Renormalization of Open QFT

Master's Thesis: Final Report

Subhobrata Chatterjee

Supervisor: Dr. R. Loganayagam and Dr. Sayantani Bhattacharya

A document submitted in partial fulfillment of the requirements of Integrated Masters' in
Physics
at
NISER, JATNI

ACKNOWLEDGEMENT

I would like to thank Dr. R. Loganayagam and Dr. Sayantani Bhattacharya for giving me a chance to work on this wonderful topic for the past fourteen months. I would also like to thank ICTS S N Bhatt Program for giving me the opportunity to start this work with Dr. Loganayagam over the summer of 2018. I thoroughly enjoyed learning about various ideas in the newly emerging area of open quantum field theory. I gained a great deal from all the discussions I had not only with my supervisors but with both NISER and ICTS faculties, students as well as my most patient, helpful and encouraging friends and seniors. Finally I owe this project to the overwhelming love and support of my parents and my dear grandparents.

Subhobrata Chatterjee

Integrated Master's student

Roll no: 1411088

NISER, Jatni

ABSTRACT

In this report, we will begin by briefly reviewing some basic background in Feynman-Vernon and Schwinger-Keldysh formalisms. Thereafter we will describe the results of some triangle one-loop calculations in scalar open SK theory. We find that the triangle (C-type) diagrams have non-local divergence similar to the divergence in cut B-type diagrams that were observed earlier. We also generalize our analysis to arbitrary one-loop diagram in open scalar field theories. This allows us to understand the structure of these novel divergences in full generality. In the last section we provide some concrete results of our analysis. We conclude with current outlook and reflect on some exciting future directions.

CONTENTS

1	INTRODUCTION TO OPEN QFT	1
1.1	Motivation	1
1.2	What is an Open QFT?	1
1.3	Feynman-Vernon Influence Functional Formalism	2
1.4	Schwinger-Keldysh Path Integral Formalism	6
1.5	Effective Field Theory from Microscopic theory	7
1.6	Markovian approximation and the Linblad condition	7
1.7	Steps in building an Open QFT	9
2	OPEN ϕ^4 SCALAR SK EFFECTIVE THEORY	11
2.1	The Effective Action	11
2.2	Diagrammatics	11
2.3	Non-local divergences in B -type diagrams in 4 dimensions	11
2.4	Explicit computation of C -type triangle diagrams	13
2.4.1	Single-cut C -type diagram	13
2.4.2	Double-cut C -type diagram	15
2.4.3	Triple cut C -type diagram	19
3	NON-LOCAL DIVERGENCE AT ONE-LOOP IN OPEN SCALAR FIELD THEORIES	23
3.1	Cut-free	25
3.2	Single cut	27
3.3	Multiple cut	29
4	DISCUSSION OF RESULTS	39
4.1	Superficial degree of divergence of cut integrals	39
4.2	Non-locality of UV divergences from non-unitary cuts	41
4.2.1	Why are one-loop UV divergences of closed QFTs local?	41
4.2.2	How is delta function responsible for UV divergence non-locality?	42
4.3	Multiple-cut UV divergence and the null plane of cut-cut external momenta	42
4.4	Structure of non-local divergence across various dimensions	44
4.5	Diagram with atleast one unitary cut is always finite	45
5	OUTLOOK AND FUTURE DIRECTIONS	47

1 INTRODUCTION TO OPEN QFT

In this section we will briefly discuss the need to formulate an open quantum field theory and also discuss two of most prominent formalisms that addressed some of the important physics underlying open systems.

1.1 MOTIVATION

Effective field theories (EFTs) have been ubiquitous in modern day theoretical physics. The success of EFTs is wide ranging with applications in particle physics, cosmology, theory of critical phenomena, polymer physics etc. The concepts and techniques of renormalisation has been key to understanding the scale dependence of coupling constants among others.

However, many a times the effective field fails to capture important physical phenomena like dissipation and information loss. This could happen for example if the system is in contact with some environment and hence is really open. Or the system is “effectively” open in that coarse graining has traced out some degrees of freedom into which the system dissipates. These situations call for some quantum field theory of mixed states, where we can trace out some degrees of freedom. Further, we can set up a renormalisation flow and study various gauge-gravity dualities.

1.2 WHAT IS AN OPEN QFT?

An open system is a system that is in contact with some environment. An open QFT is an effective quantum field theory which is obtained from an underlying unitary theory of system and environment by tracing out environment degrees of freedom. Unitarity is broken while moving from the microscopic theory of the system and environment to the effective theory of the system. The unitarity violating property of such an effective theory is what makes the physics rich and interesting.

We will now briefly review the two seminal formalisms that provide the foundations of modern ideas in open QFT viz. Feynman-Vernon and Schwinger-Keldysh.

1.3 FEYNMAN-VERNON INFLUENCE FUNCTIONAL FORMALISM

This formalism [4] was originally developed in a quantum mechanical setting although can be easily generalized to quantum field theory. We consider a system(S) coupled to an environment(or bath)(B). Following usual conventions, the system will be described by the coordinate Q while the bath labelled by the coordinate X . We describe the dynamics of the system coupled to the bath via a density matrix that evolves with time. The system bath coupling induces what is called an influence functional on the system(also called the Feynman-Vernon influence functional) after the environment degrees of freedom are traced out.

We will now give a short derivation of the Feynman-Vernon influence functional given the initial density matrix of the combination of system and its environment. Let ρ_{SB} be the density matrix of the combination.

The Liouville-von-Neumann equation gives the evolution for the density matrix (here in Schrodinger picture) with time as

$$i\hbar \frac{d}{dt} \rho_{SB}(t) = [H, \rho_{SB}(t)] \quad (1.1)$$

The solution to the above differential equation can be given once the density matrix is known at time say, $t = 0$

$$\rho_{SB}(t) = U \rho_{SB}(0) U^\dagger \quad (1.2)$$

where the unitary time evolution operator U is the given by following Dyson series

$$U = \mathcal{T} \left[e^{-\frac{i}{\hbar} \int_0^t d\tau H(\tau)} \right] \quad (1.3)$$

The \mathcal{T} in the above expression is the time-ordering operator and is crucial as the Hamiltonian can in general be time-dependent and may not commute at different times. The Hamiltonian itself can be written as a sum of three different operators,

$$H = H_S + H_B + H_{SB} \quad (1.4)$$

where H_S is the system's self Hamiltonian, H_B is the bath/environment Hamiltonian and H_{SB} is the Hamiltonian that describes the interaction between the system and the bath.

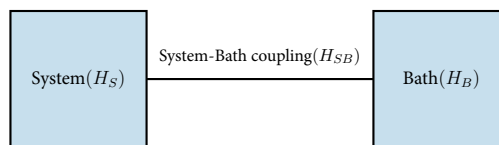


Figure 1.1: Schematic showing the interaction of a system with its environment/bath

Now the Feynman-Vernon formalism is essentially based on expressing the matrix element of the density operator of the system only(reduced density matrix), obtained by tracing out bath degrees of freedom, as a double path integral(propagator) over system and bath state variables. The double copy of state variables turns up because the density matrix with its ket and bra evolves separately in each of them. The ket component evolves forward in time while the bra component evolves backward in time. Mathematically we have,

$$\begin{aligned}
 \langle Q, t | \rho_S(t) | Q', t \rangle &= Tr_B \langle Q, X, t | \rho_{SB}(t) | Q', X', t \rangle & (1.5) \\
 &= \int \underbrace{dQ_0 dQ'_0}_{\text{initial system state differentials}} \underbrace{dX_0 dX'_0}_{\text{initial bath state differentials}} \underbrace{dX}_{\text{final bath state differential}} \times \\
 &\quad \underbrace{\langle Q, X, t | T \left[e^{-\frac{i}{\hbar} \int_0^t H(\tau) d\tau} \right] | Q_0, X_0, 0 \rangle}_{\text{right propagator}} \underbrace{\langle Q'_0, X'_0, 0 | T \left[e^{\frac{i}{\hbar} \int_0^t H(\tau) d\tau} \right] | Q', X, t \rangle}_{\text{left propagator}} \times \\
 &\quad \underbrace{\langle Q_0, X_0, 0 | \rho_{SB}(0) | Q'_0, X'_0, 0 \rangle}_{\text{initial state density matrix element}} & (1.6)
 \end{aligned}$$

From the above expressions we find that there are five integrals, four over the possible initial system and bath states and one over the final bath state. The integrand is made up of the left and right propagators and the initial state density matrix. The propagators serve to evolve the initial density matrix state(double copy) and then the outer integrals integrate over all possible initial(system,bath) and final(bath) states. Now the left and right propagators can be neatly expressed as path integrals over system and bath state variables

$$\text{right propagator} = \int_{Q_1(0)=Q_0, X_1(0)=X_0}^{Q_1(t)=Q, X_1(t)=X} \mathcal{D}Q_1 \mathcal{D}X_1 e^{\frac{i}{\hbar} (S_S[Q_1] + S_B[X_1] + S_{SB}[Q_1, X_1])} \quad (1.7)$$

$$\text{left propagator} = \langle Q', X, t | T e^{-\frac{i}{\hbar} \int_0^t H(\tau) d\tau} | Q'_0, X'_0, 0 \rangle^* \quad (1.8)$$

$$= \int_{Q_2(0)=Q'_0, X_2(0)=X'_0}^{Q_2(t)=Q', X_2(t)=X} \mathcal{D}Q_2 \mathcal{D}X_2 e^{-\frac{i}{\hbar} (S_S[Q_2] + S_B[X_2] + S_{SB}[Q_2, X_2])} \quad (1.9)$$

where $S_S[Q_1]$, $S_B[X_1]$, $S_{SB}[Q_1, X_1]$ are the actions corresponding to the system, bath and system-bath coupling Hamiltonians. Observe that the right propagator evolves the the state $|Q_0, X_0, 0\rangle$ forward in time i.e. from 0 to some time t , while the left propagator evolves the state $\langle Q'_0, X'_0, 0|$ forward in time i.e. from 0 to t . Thus in the right propagator the ket evolves forward in time(and the bra evolves backward in time), while in the left propagator the bra evolves forward in time(and the ket evolves backward in time).

1 Introduction to Open QFT

Now, we will briefly introduce the idea of influence functional. We assume a factorising initial condition of the density matrix that

$$\rho_{SB}(t=0) = \rho_S(0) \otimes \rho_B(0) \quad (1.10)$$

Then we can re-write (1.6) in a form that suggests integrating out the environment variables first

$$\langle Q, t | \rho_S(t) | Q', t \rangle = \int dQ_0 dQ'_0 \langle Q_0, 0 | \rho_S(0) | Q'_0, 0 \rangle \int_{Q_1(0)=Q_0, Q_2(0)=Q'_0}^{Q_1(t)=Q, Q_2(t)=Q'} \mathcal{D}Q_1 \mathcal{D}Q_2 e^{\frac{i}{\hbar}(S_S[Q_1] - S_S[Q_2])} \mathcal{F}[Q_1, Q_2] \quad (1.11)$$

where $\mathcal{F}[Q_1, Q_2]$ is called the influence functional and is given by

$$\mathcal{F}[Q_1(t), Q_2(t)] \equiv \int_{X_1(0)=X_0, X_2(0)=X'_0}^{X_1(t)=X_2(t)=X} dX_0 dX'_0 dX \langle X_0, 0 | \rho_B(0) | X'_0, 0 \rangle \times \int \mathcal{D}X_1 \mathcal{D}X_2 e^{\frac{i}{\hbar}(S_B[X_1] + S_{SB}[Q_1, X_1] - S_B[X_2] - S_{SB}[Q_2, X_2])} \quad (1.12)$$

The influence functional involves double path integral over the ket and bra bath variables from some initial state (X_0, X'_0) to a common final state (X). The initial and final state variables are thereafter integrated out to give an expression that is only a function of the ket and bra system variables. The action of the double path integral involves both the bath as well as the system-bath coupling and hence the influence functional measures the coupling between the system and the bath over all possible bath state evolution. If the influence functional \mathcal{F} is defined to be $e^{\frac{i}{\hbar} S_{FV}[Q_1(t), Q_2(t)]}$ then we can call $S_{FV}(Q_1(t), Q_2(t))$ the corresponding influence phase.

Thus, the influence phase/functional obtained by coarse-graining the bath describes the effect of the bath on the time-evolution of the system density matrix (1.11). It's a functional in that it takes in the histories of the ket and bra states of the system and spits out a number that tells how differently they evolved over time under the influence of the environment.

In [4, section C], Feynman and Vernon list five basic properties of influence functionals. We list them below:

1. Averaging rule: If the physical situation is not known completely (as for instance if the type of environment X , or the initial or final states are not known precisely) but if the probability of the p th situation is w_p and the corresponding influence functional is \mathcal{F}_p , then the effective \mathcal{F} is given by

$$\mathcal{F}_{eff} = \sum_p w_p \mathcal{F}_p \equiv \langle \mathcal{F} \rangle \quad (1.13)$$

2. Product rule: If a number of statistically and dynamically independent partial systems act on Q at the same time and $\mathcal{F}^{(k)}$ is the influence of the k th system alone, the total influence of all is given by the product of individual $\mathcal{F}^{(k)}$:

$$\mathcal{F} = \prod_{k=1}^N \mathcal{F}^{(k)} \quad (1.14)$$

3. Conjugate Symmetry: The influence functional has the property that

$$\mathcal{F}^*(Q, Q') = \mathcal{F}(Q, Q') \quad (1.15)$$

which can easily be seen from its definition in (1.12).

4. Independence of system state history I(weaker): In the class of problems in which the final state of the bath is arbitrary, which means that the final states are to be summed over, then $\mathcal{F}(Q, Q')$ is independent of $Q(t)$ if $Q(t) = Q'(t)$ for all t . From the definition in (1.12), it follows that the influence functional can be written as a trace

$$\begin{aligned} \mathcal{F}[Q_1(t), Q_2(t)] &= \int dX_0 dX'_0 dX \langle X_0 | \rho_B | X'_0 \rangle \langle X | U_B[Q_1(t)] | X_0 \rangle \langle X | U_B[Q_2(t)] | X'_0 \rangle^* \\ &= \text{Tr}_B \left(\rho_B U_B^\dagger[Q_2(t)] U_B[Q_1(t)] \right) \end{aligned} \quad (1.16)$$

where $U_B[Q(t)]$ is the time-evolution operator for the time-dependent Hamiltonian $H_B + H_{SB}[Q(t)]$

From (1.16), if $Q_1(t)$ and $Q_2(t)$ paths are equal at all times then the influence functional becomes unity

$$Q_1(t) = Q_2(t) \implies \mathcal{F}[Q_1(t), Q_2(t)] = 1 \quad (1.17)$$

Thus, the influence functional doesn't contribute to the reduced density matrix evolution of the system for equal ket and bra state histories. This in turn means that the environment has no effect on the system in the coarse-grained picture.

5. Independence of system state history II(stronger): The stronger version of the previous property is that when final bath states are summed up, if $Q(t) = Q'(t)$ for all $t > r$ then $\mathcal{F}(Q, Q')$ is independent of $Q(t)$ for $t > r$. For linear driven systems, this property leads to statements about causality.

1.4 SCHWINGER-KELDYSH PATH INTEGRAL FORMALISM

Schwinger-Keldysh formalism([8],[6]) is also a path integral formulation of the evolution of density matrix(for describing mixed states) that originally arose in the description of many-body non-equilibrium systems. The dynamics of any system is described by a pair of fields, ket(or right) field ϕ_R and bra(or left) field ϕ_L . One can write the generating function for all correlation functions(with one time-ordering violation) as:

$$\mathcal{Z}_{SK}[J_R, J_L] = \text{Tr} (U[J_R]\rho_i U[J_L]^\dagger) \quad (1.18)$$

where $U[J]$ is the unitary evolution operator for the quantum field theory deformed by sources J for some operators of the theory.

Given an action $S[\phi, J]$ of a unitary QFT, one can write a path integral representation of the of $\mathcal{Z}_{SK}[J_R, J_L]$:

$$\mathcal{Z}_{SK}[J_R, J_L] = \int_{\rho_i(\phi_R, \phi_L)}^{\phi_R|_{t=\infty}=\phi_L|_{t=\infty}} [\mathcal{D}\phi_R][\mathcal{D}\phi_L] e^{i(S[\phi_R, J_R]-S[\phi_L, J_L])} \quad (1.19)$$

The lower limit is the statement that near $t = t_i$ the boundary condition for the path integral is weighed by the initial density matrix ρ_i . The upper limit is the statement that the bra and the ket fields should be set equal at far future and summed over in order to correctly reproduce the trace. The factors $e^{iS[\phi_R, J_R]}$ and $e^{-iS[\phi_L, J_L]}$ correctly reproduce the evolution operators $U[J_R]$ and $(U[J_L])^\dagger$ respectively. As can be seen from the above expression that the Schwinger-Keldysh action for a unitary theory is given by

$$S_{SK} = S[\phi_R] - S[\phi_L] \quad (1.20)$$

If the unitary QFT is in perturbative regime, the above path integral can be used to set up Veltman rules([9]):

1. In a unitary QFT, there are no vertices coupling the bra and the ket fields. The bra vertices are complex conjugates of ket vertices.
2. The ket propagator is time-ordered while the bra propagator is anti-time-ordered. The SK boundary conditions also induce a bra-ket propagator which is the on-shell propagator(obtained by putting the exchanged particle on-shell). These propagators are called cut propagators(for formula see [section 2.1](#)). The term ‘‘cut’’ is inspired from Cutkosky cutting rules([3]) where one thinks of the dividing line between the bra and ket parts of a diagram as a ‘‘cut’’ of a diagram where particles go on-shell.

1.5 EFFECTIVE FIELD THEORY FROM MICROSCOPIC THEORY

Now, we consider an open system where a system is coupled to its environment. Let's consider ϕ to be the system field while χ to be the environment field. In the Schwinger-Keldysh formalism now we have to work with doubled degrees of freedom that we distinguish by “left” and “right”. Let ϕ_L, ϕ_R be the left and right fields of the system while χ_L, χ_R be the left and right fields of the environment.

We can construct the SK path integral for the “system+environment” combination as follows:

$$\mathcal{Z}_{SK} = \int [\mathcal{D}\phi_R][\mathcal{D}\chi_R][\mathcal{D}\phi_L][\mathcal{D}\chi_L] e^{i(S[\phi_R, \chi_R] - S[\phi_L, \chi_L])} \quad (1.21)$$

The above generating function contains microscopic data about the interactions between the system and the environment. However, in practice the environment may have extremely complicated microscopic dynamics yet have a simple macroscopic influence on the system. The effective field theory formalism helps us coarse grain the environment degrees of freedom and package the otherwise messy data into a “coupling action” for the effective theory of the system. This “coupling action” in QFT lingo is nothing but the Feynman-Vernon influence phase we discussed in the first section.

If we trace out the left and right χ fields, we obtain an effective action that looks like:

$$S_{\text{effective}} = S[\phi_R] - S[\phi_L] + S_{FV}[\phi_R, \phi_L] \quad (1.22)$$

where S_{FV} describes the system-environment coupling in terms only system's left and right field coupling.

The presence of the S_{FV} term lends non-unitary character to the effective theory of the system starting from a unitary theory of system and environment.

1.6 MARKOVIAN APPROXIMATION AND THE LINBLAD CONDITION

In the case of coherent evolution, we find it very convenient to characterize the dynamics of a quantum system with a Hamiltonian, which describes the evolution over an infinitesimal time interval. The dynamics is then described by a differential equation, the Schrodinger equation, and we may calculate the evolution over a finite time interval by integrating the equation, i.e. by piecing together the evolution over many infinitesimal intervals. Even if the evolution is not coherent, it is often possible to describe the evolution of a density matrix, at least to a good approximation, by a differential equation. This equation, is what is called the quantum master equation. The fact that a linear differential equation can capture a good deal of the rich physics, is based upon the fundamental notion of markovianity, which means being local in time. If the

1 Introduction to Open QFT

evolution of the density matrix $\rho(t)$ is governed by a (first-order) differential equation in t , then that means that $\rho(t + dt)$ is completely determined by $\rho(t)$.

In general the density matrix $\rho_S(t + dt)$ can depend not only on $\rho_S(t)$, but also on ρ_S at earlier times, because the environment retains a memory of this information for a while, and can transfer it back to the system. An open system(whether classical or quantum) is dissipative because information can flow back from reservoir to system, resulting in non-markovian fluctuations of the system.

Still, in most contexts, a markovian description entails a very good approximation. The key idea is that there may be a clean separation between the typical correlation time of the fluctuations and the time scale of the evolution we want to follow. Crudely speaking, we may denote by δt_E the time it takes for the environment to to “forget” information that it acquired from the system. After time δt_E we can regard that information as forever lost, and neglect the possibility that the information may feedback again to influence the subsequent evolution of the system. Our description of the evolution of the system will incorporate coarse-graining in time; we perceive the dynamics through a filter that screen out the high frequency components of the motion, with $\omega \gg \frac{1}{\delta t_{coarse}}$. An approximate markovian description should be possible then, if $\delta t_E \ll \delta t_{coarse}$; we can neglect the memory of the environment, because we are unable to resolve its effects. This “markovian approximation” will be useful if the time scale of the dynamics that we want to observe is long compared to δt_{coarse} , e.g., if the damping time scale δt_{damp} satisfies $\delta t_{damp} \gg \delta t_{coarse} \gg \delta t_E$.

This leads us to ask the question of whether we can generalize the quantum Liouville equation, $\dot{\rho} = -i[H, \rho]$, that describes the time-evolution of density matrix for a closed system to the case of markovian but non-unitary evolution, for which we will have $\dot{\rho} = \mathcal{L}[\rho]$, for some linear operator \mathcal{L} . The answer is yes! This was the famous work of the quartet Gorini, Kossakowski, Suadarshan and Linblad and hence goes by the name GKSL equation(from their initials), or the Linblad equation in short. The linear operator \mathcal{L} , which generates a finite superoperator(operator acting on an operator) in that same sense that a Hamiltonian H generates unitary time evolution, will be called the Lindbladian.

The Linblad equation (in diagonal form) in Schrodinger picture looks like

$$\dot{\rho}(t) = \mathcal{L}[\rho] = -i[H, \rho(t)] + \sum_k \gamma_k \left(L_k \rho(t) L_k^\dagger - \frac{1}{2} \{L_k^\dagger L_k, \rho(t)\} \right) \quad (1.23)$$

L_i are a linear basis of operators acting on the system’s Hilbert space and are called Linblad or jump operators, and γ_k are non-negative constants which determine the dynamics due to system-environment coupling. It follows from the above equation that the evolution is trace preserving i.e

$$\frac{d}{dt}(\text{tr } \rho) = 0 \quad (1.24)$$

From the above form (1.23), we can see that time evolution of the density matrix of the system has two parts. The first term is the unitary part of the dynamics generated by the (Hermitian) Hamiltonian H and the second term describes the non-unitary part of the dynamics that is due to the system's interaction with its environment. Each $L_k \rho L_k^\dagger$ term induces one of the possible quantum jumps, while the $-\frac{1}{2}\{L_k^\dagger L_k, \rho\}$ term is needed to normalize properly the case where no jumps occur.

The Lindblad equation above can also be expressed in Heisenberg picture. If X is a quantum observable, then its Lindblad equation in Heisenberg picture is

$$\dot{X} = i[H, X] + \sum_k \gamma_k \left(L_k^\dagger X L_k - \frac{1}{2} \{L_k^\dagger L_k, X\} \right) \quad (1.25)$$

Further, the Lindbladian can be incorporated into the path-integral language, by adding an a Feynman-Vernon influence functional to the Schwinger-Keldysh action of the system.

$$S_{FV} = i \int \sum_{\alpha, \beta} \Gamma_{\alpha, \beta} \left(L_\alpha^\dagger[\phi_R] L_\beta[\phi_L] - \frac{1}{2} L_\alpha^\dagger[\phi_R] L_\beta[\phi_R] - \frac{1}{2} L_\alpha^\dagger[\phi_L] L_\beta[\phi_L] \right) \quad (1.26)$$

where L_α are a set of operators and $\Gamma_{\alpha, \beta}$ are the system-environment couplings that determine the non-unitary dynamics of the system. This means that the Lindblad condition imposes severe restrictions on the form of the Feynman-Vernon term in the Schwinger-Keldysh effective action, provided the underlying system respects markovianity. The Feynman-Vernon(FV) couplings induced by integrating out environment fields in a effective theory need not always be local. A description of the resultant open QFT is often achieved by time scales for environment fluctuations are typically very fast as compared to the information flow rate from the system to the environment itself. In this approximation, one expects a nice local non-unitary EFT, possibly respecting the field theoretic analogue of the Lindblad condition.

This concludes our brief discussion of the background ideas involved in the formulation of an open QFT. We will now elucidate the recipe to do open QFT.

1.7 STEPS IN BUILDING AN OPEN QFT

Given the background, we can now construct an open QFT by going through the following steps:

1. Schwinger-Keldysh(SK) path integrals: We first write down an SK action for doubled degrees of freedom(for describing both left and right moving states). For unitary QFT, the SK action is just the difference of the right and left self-actions. The SK path integrals depend on initial state of system and environment and the left and right fields are set equal to each other in the far future. We compute the generating function for the theory deformed by doubled sources. By taking derivatives of the generating function wrt the sources we can easily calculate correlation functions(with atmost one time-ordering violation).

1 Introduction to Open QFT

2. Veltman Rules: For unitary SK theory, Feynman rules for diagrammatics get lifted to generalized Veltman rules whereby one has cut propagators in addition to usual propagators. The cut propagators are nothing but the coupling of the ket and bra fields at the level of propagators. They are on-shell propagators along which a ket state freely transforms into a bra state and vice versa. They come equipped with a prescribed direction of energy flow. Since the unitary SK action looks like $S_{SK} = S[\phi_R] - S[\phi_L]$, there cannot be a cut vertex in unitary SK theory.
3. Feynman-Vernon coupling: In coarse graining environment degrees of freedom from an underlying microscopic theory, new terms appear that encode coupling information between the system and the environment. These new influence functional terms mix the bra and ket fields and give rise to an open QFT. The Veltman rules get extended to include cut vertices in addition to cut propagators.

$$\text{---} \times \text{---} = \left(\text{---} \times \overset{\text{Env}}{\text{---}} \times \text{---} \right)_{\text{Unitary QFT}}$$

Figure 1.2: Generating a cut vertex ala Feynman-Vernon

4. Lindblad structure: Just as many markovian quantum mechanical systems obey the Lindblad condition, there may be certain open quantum field theories (with constrained couplings) for which Lindblad condition may be respected. More so, if the Feynman-Vernon action is due to a Lindbladian, the question of protection of Lindblad structure under RG flow is an extremely pertinent one.

2 OPEN ϕ^4 SCALAR SK EFFECTIVE THEORY

2.1 THE EFFECTIVE ACTION



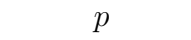
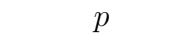
As described in [1], one can write down the action for the most general open quantum field theory, consisting of a real scalar which can interact via cubic and quartic interactions (taking into account CPT symmetry and SK boundary conditions):

$$\begin{aligned}
S = & - \int d^d x \left[\frac{1}{2} z (\partial \phi_R)^2 + \frac{1}{2} m^2 \phi_R^2 + \frac{\lambda_4}{4!} \phi_R^4 + \frac{\sigma_4}{3!} \phi_R^3 \phi_L \right] \\
& + \int d^d x \left[\frac{1}{2} z^* (\partial \phi_L)^2 + \frac{1}{2} (m^2)^* \phi_L^2 + \frac{\lambda_4^*}{4!} \phi_L^4 + \frac{\sigma_4^*}{3!} \phi_L^3 \phi_R \right] \\
& + i \int d^d x \left[z_\Delta (\partial \phi_R) \cdot (\partial \phi_L) + m_\Delta^2 \phi_R \phi_L + \frac{\lambda_\Delta}{2!2!} \phi_R^2 \phi_L^2 \right] \\
& - \int d^d x \left[\frac{\lambda_3}{3!} \phi_R^3 - \frac{\lambda_3^*}{3!} \phi_L^3 + \frac{\sigma_3}{2!} \phi_R^2 \phi_L - \frac{\sigma_3^*}{2!} \phi_L^2 \phi_R \right]
\end{aligned} \tag{2.1}$$

We will look at the Feynman diagrams at one loop for the above theory.

2.2 DIAGRAMMATICS

Let solid and dotted stand for ϕ_R and ϕ_L respectively while blue and red stand for uncut and cut propagators respectively. The Veltman rules for the propagators in the open scalar $\phi^3 + \phi^4$ theory will now be listed.

- Right propagator(R): $\langle \phi_R(-p) \phi_R(p) \rangle = \frac{-i}{p^2 + m^2 - i\epsilon}$ 
- Left propagator(L): $\langle \phi_L(-p) \phi_L(p) \rangle = \frac{i}{p^2 + m^2 + i\epsilon}$ 
- Plus propagator(P): $\langle \phi_R(-p) \phi_L(p) \rangle = 2\pi\theta(p^0)\delta(p^2 + m^2)$ 
- Minus propagator(M): $\langle \phi_L(-p) \phi_R(p) \rangle = 2\pi\theta(-p^0)\delta(p^2 + m^2)$ 

2.3 NON-LOCAL DIVERGENCES IN B -TYPE DIAGRAMS IN 4 DIMENSIONS

In [1, appendix A], the authors call the tadpole diagrams obtained using various combinations of the four propagators(R,L,P,M) as $B_{\langle \text{prop. 1} \rangle, \langle \text{prop. 2} \rangle}$ where $\langle \cdot \rangle$ is one of the labels R,L,P or M. The

2 Open ϕ^4 scalar SK effective theory

naming convention is based on propagator counting starting from the left bottom vertex and moving in the counter-clockwise direction. There are 16 six diagrams if the masses of the two propagators are taken to be different in general.

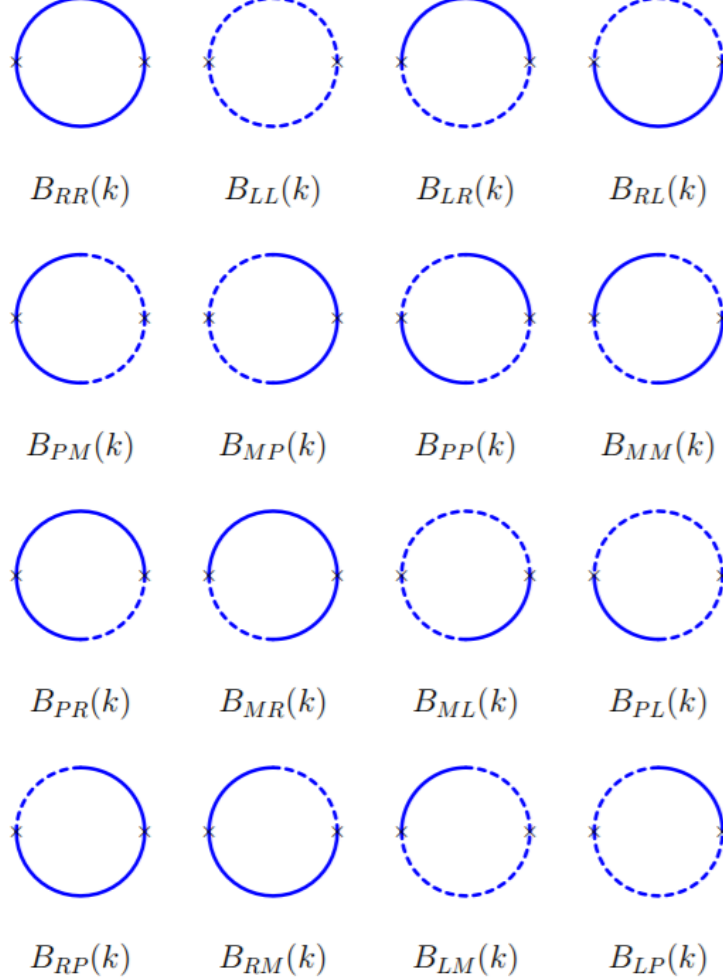


Figure 2.1: List of all possible B-type diagrams with different masses for the two propagators(see [1, appendix A])

The divergent Passarino-Veltman B-type diagrams together with their divergent structures were identified to be([1, appendix B.5.3]):

$$\begin{aligned}
 \text{div}[B_{RP}] \Big|_{\overline{MS}} &= \text{div}[B_{RM}] \Big|_{\overline{MS}} = \frac{i}{(4\pi)^2} \frac{k^2 - \bar{m}^2 + m^2}{2k^2} \left[\frac{2}{d-4} + \ln \left(\frac{1}{4\pi e^{-\gamma_E}} \right) \right] \\
 \text{div}[B_{PR}] \Big|_{\overline{MS}} &= \text{div}[B_{MR}] \Big|_{\overline{MS}} = \frac{i}{(4\pi)^2} \frac{k^2 + \bar{m}^2 - m^2}{2k^2} \left[\frac{2}{d-4} + \ln \left(\frac{1}{4\pi e^{-\gamma_E}} \right) \right] \\
 \text{div}[B_{RL}] \Big|_{\overline{MS}} &= \text{div}[B_{LR}] \Big|_{\overline{MS}} = \frac{i}{(4\pi)^2} \frac{m^2 - \bar{m}^2}{2k^2} \left[\frac{2}{d-4} + \ln \left(\frac{1}{4\pi e^{-\gamma_E}} \right) \right] \\
 \text{div}[B_{RR}] \Big|_{\overline{MS}} &= \text{div}[B_{LL}] \Big|_{\overline{MS}} = \frac{i}{(4\pi)^2} \left[\frac{2}{d-4} + \ln \left(\frac{1}{4\pi e^{-\gamma_E}} \right) \right]
 \end{aligned} \tag{2.2}$$

2.4 Explicit computation of C -type triangle diagrams

When masses were set equal $\bar{m} = m$, the divergence structures of the “quarter-cut” diagrams reduce to:

$$\begin{aligned} \text{div}[B_{RP}] \Big|_{\overline{MS}} &= \text{div}[B_{PR}] \Big|_{\overline{MS}} = \text{div}[B_{RM}] \Big|_{\overline{MS}} = \text{div}[B_{MR}] \Big|_{\overline{MS}} = \frac{i}{2(4\pi)^2} \left[\frac{2}{d-4} + \ln \left(\frac{1}{4\pi e^{-\gamma_E}} \right) \right] \\ \text{div}[B_{LP}] \Big|_{\overline{MS}} &= \text{div}[B_{PL}] \Big|_{\overline{MS}} = \text{div}[B_{LM}] \Big|_{\overline{ML}} = \text{div}[B_{ML}] \Big|_{\overline{MS}} = -\frac{i}{2(4\pi)^2} \left[\frac{2}{d-4} + \ln \left(\frac{1}{4\pi e^{-\gamma_E}} \right) \right] \end{aligned} \quad (2.3)$$

For $\bar{m} = m$, B_{RL} and B_{LR} become finite while B_{RR} and B_{LL} divergences now turn out to be exactly double of the B_{RP} divergence.

It was thus found that the B-type diagrams have local divergence (divergence structure polynomial in external momenta) only when $\bar{m} = m$. However, when the masses are unequal B_{RP} , B_{PR} , B_{RL} and other the related diagrams have non-local divergence $\propto \frac{1}{k^2}$. This sparked an interest to explore and understand the origin of such divergences in this theory and more generally in open QFTs.

In this report, in an effort to try to understand these divergences systematically we are extending the study to triangle one-loop diagrams which we call C-type. For understanding the structure of divergences, we will consider two generic external momenta (third one fixed by momentum conservation) and three generic masses for the three internal lines.

2.4 EXPLICIT COMPUTATION OF C -TYPE TRIANGLE DIAGRAMS

In this section we compute the non-local divergences across all three kinds of C-type diagrams viz. single cut, double cut and triple cut in four spacetime dimensions. The calculations are a bit tricky as we do not have the luxury of using Wick rotation due to the presence of delta functions. We use cut-off regularization to extract the divergences in these diagrams.

2.4.1 SINGLE-CUT C -TYPE DIAGRAM

Here we will compute a single-cut C -type diagram viz. C_{PRR} in 4 spacetime dimensions. The integral expression is

$$C_{PRR}(k_1, k_3) = (-i)^2 \int \frac{d^4 p}{(2\pi)^4} \frac{2\pi \Theta(p^0) \delta(p^2 + m_1^2)}{[(p + k_1)^2 + m_2^2 - i\varepsilon][(p - k_3)^2 + m_3^2 - i\varepsilon]} \quad (2.4)$$

We have kept the propagators to be of different masses for generality. In the end we can set them to be equal.

The diagram corresponding to C_{PRR} is shown in figure (2.2).

2 Open ϕ^4 scalar SK effective theory

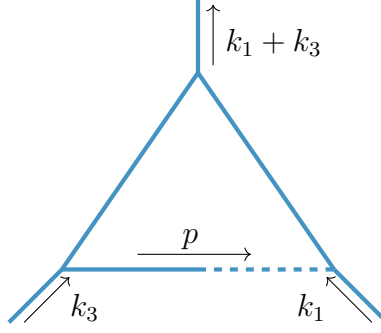


Figure 2.2: C_{PRR}

Firstly, note the following identity:

$$\delta_+(p^2 + m_1^2) = \frac{\delta(p^0 - \omega_p)}{2\omega_p}; \quad \omega_p \equiv \sqrt{\mathbf{p}^2 + m_1^2} \quad (2.5)$$

Using (2.5) in (2.4) we get

$$C_{PRR} = - \int \frac{d^3p}{(2\pi)^3 2\omega_p} \times \frac{1}{((p + k_1)^2 + m_2^2 - i\varepsilon)|_{p^0=\omega_p} ((p - k_3)^2 + m_3^2 - i\varepsilon)|_{p^0=\omega_p}} \quad (2.6)$$

Now we will Feynman parametrisation to club the two propagators into one.

$$C_{PRR} = - \int \frac{d^3p}{(2\pi)^3 2\omega_p} \int_0^1 \frac{dx}{(p^2 + 2k_{13} \cdot p + \Delta_{13})^2|_{p^0=\omega_p}}, \quad (2.7)$$

where

$$\begin{aligned} \Delta_{13} &\equiv (k_1^2 + m_2^2)x + (k_3^2 + m_3^2)(1 - x) - i\varepsilon, \\ k_{13} &\equiv k_1x - k_3(1 - x). \end{aligned} \quad (2.8)$$

We now substitute $p^0 = \omega_p$ explicitly in (2.7) and express the loop momentum in spherical polar coordinates. The angle between \mathbf{k}_{13} and \mathbf{p} is taken to be θ .

$$\begin{aligned} C_{PRR} &= - \frac{1}{(2\pi)^2} \int_0^1 dx \int_0^\infty \frac{|\mathbf{p}^2| d|\mathbf{p}|}{2\omega_p} \int_0^\pi \frac{\sin \theta d\theta}{(-m_1^2 - 2k_{13}^0 \omega_p + 2|\mathbf{k}_{13}||\mathbf{p}| \cos \theta + \Delta_{13})^2} \\ &= - \frac{1}{(2\pi)^2} \int_0^1 dx \int_0^\infty \frac{|\mathbf{p}^2| d|\mathbf{p}|}{\omega_p (-m_1^2 - 2k_{13}^0 \omega_p + \Delta_{13} - 2|\mathbf{k}_{13}||\mathbf{p}|) (-m_1^2 - 2k_{13}^0 \omega_p + \Delta_{13} + 2|\mathbf{k}_{13}||\mathbf{p}|)} \\ &= - \frac{1}{(2\pi)^2} \int_0^1 dx \int_{m_1}^{\omega_p} \frac{(\omega_p^2 - m_1^2)^{\frac{1}{2}} d\omega_p}{(m_1^2 + 2k_{13}^0 \omega_p - \Delta_{13})^2 - 4|\mathbf{k}_{13}|^2 (\omega_p^2 - m_1^2)} \end{aligned} \quad (2.9)$$

2.4 Explicit computation of C -type triangle diagrams

Now, we will compute the integral in the large ω_p regime i.e. over the domain where ω_p is much larger than all masses and the external momenta.

$$\frac{1}{(4\pi)^2} \int_{m_1}^{\infty} d\omega_p \left(\frac{1}{\omega_p} \int_0^1 \frac{dx}{k_{13}^2} + \mathcal{O}\left(\frac{1}{\omega_p^2}\right) \right) \quad (2.10)$$

The above integral diverges logarithmically. So we regularize it by putting a hard UV cutoff, Λ .¹ The closed form expression for the above integral is noted below.

$$\text{div}(C_{PRR}) = \frac{1}{(4\pi)^2} \frac{\tan^{-1}\left(\frac{\sqrt{\Sigma^2}}{-k_1 \cdot k_3}\right)}{\sqrt{\Sigma^2}} \log(\Lambda) \quad (2.11)$$

where we have defined $\Sigma^2 \equiv k_1^2 k_3^2 - (k_1 \cdot k_3)^2$.

2.4.2 DOUBLE-CUT C -TYPE DIAGRAM

Consider the double-cut C -type diagram C_{PRR} . The diagram is shown in figure (2.3) and the integral expression is

$$C_{PRR} = (-i) \int \frac{d^4 p}{(2\pi)^4} \frac{2\pi\delta_+(p^2 + m_1^2) 2\pi\delta_+((p + k_1)^2 + m_2^2)}{(p - k_3)^2 + m_3^2 - i\epsilon} \quad (2.12)$$

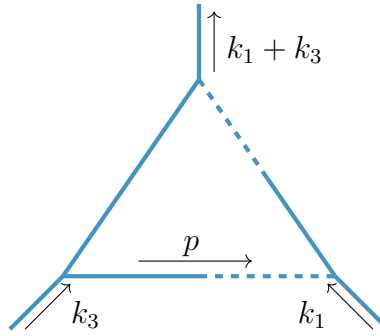


Figure 2.3: C_{PRR}

Once again we note the following identity (as used earlier in the computation of C_{PRR})

$$\delta_+(p^2 + m_1^2) = \frac{\delta(p^0 - \omega_p)}{2\omega_p}; \quad \omega_p \equiv \sqrt{\mathbf{p}^2 + m_1^2} \quad (2.13)$$

¹Note that the x integral above becomes improper when k_{13} becomes null for some isolated point between 0 and 1. In that case, the x -integral is to be treated as a Cauchy principal value integral.

2 Open ϕ^4 scalar SK effective theory

Performing the p^0 integral using the above identity we get

$$C_{PPR} = (-i) \int \frac{d^3p}{(2\pi)^3} \frac{1}{2\omega_p} \frac{2\pi\delta_+((p+k_1)^2 + m_2^2)|_{p^0=\omega_p}}{[(p-k_3)^2 + m_3^2 - i\varepsilon]|_{p^0=\omega_p}} \quad (2.14)$$

Now consider two cases:

- k_1 is space-like. In this case we find non-local log divergence.
- k_1 is time-like. In this case the answer is finite.

SPACE-LIKE k_1 :

Since k_1 is space-like, we can choose a reference frame such that the time component of k_1 is zero and k_1 is along the z direction. Further, let k_3 be at an angle θ_0 w.r.t. k_1 . Thus

$$\begin{aligned} k_1^\mu &= (0, 0, 0, |k_1|) \\ k_3^\mu &= (k_3^0, |k_3| \sin \theta_0, 0, |k_3| \cos \theta_0) \end{aligned} \quad (2.15)$$

Working in the above frame, the equation (2.14) with loop momentum in spherical polar coordinates looks like

$$\begin{aligned} C_{PPR} &= (-i) \int \frac{|p|^2 d|p| d(-\cos \theta) d\phi}{(2\pi)^2} \frac{1}{2\omega_p} \\ &\times \frac{\Theta(\omega_p) \delta(2|k_1||p| \cos \theta + k_1^2 - m_1^2 + m_2^2)}{2k_3^0\omega_p - 2(\sin \theta \cos \phi \sin \theta_0 + \cos \theta \cos \theta_0)|k_3||p| + k_3^2 - m_1^2 + m_3^2 - i\varepsilon}. \end{aligned} \quad (2.16)$$

Solving the θ integral first we get

$$\begin{aligned} C_{PPR} &= \frac{i}{2(2\pi)^2} \frac{1}{|k_1|} \int \frac{|p| d|p| d\phi}{2\omega_p} \\ &\times \frac{\Theta\left(1 - \frac{|k_1^2 - m_1^2 + m_2^2|}{2|k_1||p|}\right)}{2k_3^0\omega_p - 2(\sin \theta \cos \phi \sin \theta_0 + \cos \theta \cos \theta_0)|k_3||p| + k_3^2 - m_1^2 + m_3^2 - i\varepsilon} \Bigg|_{\cos \theta = -\frac{k_1^2 - m_1^2 + m_2^2}{2|k_1||p|}}. \end{aligned} \quad (2.17)$$

We will now perform the ϕ integral. The ϕ integral can be performed using the following standard result

$$\int_0^{2\pi} \frac{d\phi}{A \cos \phi + B} = \frac{2\pi \operatorname{csgn}(B)}{\sqrt{B^2 - A^2}} \quad (2.18)$$

where

$$\begin{aligned} B &= 2\omega_p k_3^0 + \frac{|k_3|}{|k_1|} \cos \theta_0 (k_1^2 - m_1^2 + m_2^2) + k_3^2 - m_1^2 + m_3^2 - i\epsilon \\ A &= -\sin \theta_0 \frac{|k_3|}{|k_1|} \sqrt{4|k_1|^2 |p|^2 - (k_1^2 - m_1^2 + m_2^2)^2} \end{aligned} \quad (2.19)$$

and csgn is the complex signum function.

In the high $|p|$ limit we have

$$\begin{aligned} B &\approx 2k_3^0 |p| \\ A &\approx -2 \sin \theta_0 |k_3| |p| \\ \text{csgn}(B) &\approx \text{sgn}(k_3^0) \end{aligned} \quad (2.20)$$

Hence the large momentum sector of the integral looks like

$$\frac{i\pi}{(4\pi)^2} \frac{1}{|k_1|} \int_{\Lambda_0}^{\Lambda} d|p| \left(\frac{\text{sgn}(k_3^0)}{|p| \sqrt{(k_3^0)^2 - (\sin \theta_0 |k_3|)^2}} + \mathcal{O}\left(\frac{1}{|p|^2}\right) \right) \quad (2.21)$$

The above integral is clearly logarithmically divergent. So we have put a hard cutoff Λ . The Lorentz covariant form is obtained by observing that

$$\begin{aligned} |k_1| \sqrt{(k_3^0)^2 - (\sin \theta_0 |k_3|)^2} &= |k_1| \sqrt{(k_3^0)^2 - |k_3|^2 + \cos^2 \theta_0 |k_3|^2} \\ &= \sqrt{-k_3^2 |k_1|^2 + (|k_1| \cdot |k_3|)^2} \end{aligned} \quad (2.22)$$

which from (2.15) follows that the term inside the square-root is nothing but the covariant quantity

$$-k_1^2 k_3^2 + (k_1 \cdot k_3)^2 \equiv -\Sigma^2 \quad (2.23)$$

So we get

$$\text{div}(C_{PPR}) \Big|_{\text{space-like } k_1} = \frac{i\pi}{(4\pi)^2} \frac{\text{sgn}(k_3^0)}{\sqrt{-\Sigma^2}} \log(\Lambda) \quad (2.24)$$

2 Open ϕ^4 scalar SK effective theory

TIME-LIKE k_1 :

Let us work in the rest frame of k_1 that is where $k_1^\mu = (M, 0)$. Further let $k_3^\mu = (k_3^0, 0, 0, |k_3|)$. Then the the expression for C_{PPR} (equation 2.14) when written in the above frame looks like

$$C_{PPR} = (-i) \int \frac{d^3p}{(2\pi)^3} \frac{1}{2\omega_p} \frac{2\pi\Theta(\omega_p + M) \delta(-2\omega_p M + m_2^2 - M^2 - m_1^2)}{2\omega_p k_3^0 - 2\mathbf{p} \cdot \mathbf{k}_3 + k_3^2 - m_1^2 + m_3^2 - i\varepsilon} \quad (2.25)$$

Passing to spherical polar coordinates for loop momentum and calling the angle between \mathbf{p} and \mathbf{k}_3 to be θ , we get

$$C_{PPR} = \frac{-i}{2|M|} \int_0^\infty \frac{|\mathbf{p}|^2 d|\mathbf{p}|}{(2\pi)} \frac{1}{2\omega_p} \int_0^\pi d\theta \sin\theta \frac{\Theta(\omega_p + M) \delta\left(\omega_p - \frac{m_2^2 - M^2 - m_1^2}{2M}\right)}{2\omega_p k_3^0 - 2|\mathbf{p}||\mathbf{k}_3| \cos\theta + k_3^2 - m_1^2 + m_3^2 - i\varepsilon} \quad (2.26)$$

Changing the variable $|\mathbf{p}|$ to ω_p and performing the ω_p integral with the aid of the delta function we get ²

$$C_{PPR} = \frac{-i}{8\pi|M|} \left[\Theta(\omega_p + M) \Theta(\omega_p - m_1) \sqrt{\omega_p^2 - m_1^2} \times \int_0^\pi \frac{d\theta \sin\theta}{2\omega_p k_3^0 - 2\sqrt{\omega_p^2 - m_1^2} |\mathbf{k}_3| \cos\theta + k_3^2 - m_1^2 + m_3^2 - i\varepsilon} \right] \Bigg|_{\omega_p = \frac{m_2^2 - M^2 - m_1^2}{2M}} \quad (2.27)$$

Next we perform the θ integral

$$C_{PPR} = \frac{-i}{8\pi|M|} \Theta(\omega_p + M) \Theta(\omega_p - m_1) \times \frac{1}{|k_3|} \tanh^{-1} \left(\frac{2|k_3| \sqrt{\omega_p^2 - m_1^2}}{2\omega_p k_3^0 + k_3^2 - m_1^2 + m_3^2 - i\varepsilon} \right) \Bigg|_{\omega_p = \frac{m_2^2 - M^2 - m_1^2}{2M}} \quad (2.28)$$

We can covariantize this solution by boosting back from the rest frame of k_1 to the starting frame. That amounts to substituting the following:

$$k_3^0 = -\text{sgn}(k_1^0) \frac{k_1 \cdot k_3}{\sqrt{-k_1^2}} \quad (2.29)$$

$$|k_3| = \frac{\sqrt{(k_1 \cdot k_3)^2 - k_1^2 k_3^2}}{\sqrt{-k_1^2}} \quad (2.30)$$

²The above expression picks up an extra step function, $\Theta(\omega_p - m_1)$, because of the following reason: The lower limit of ω_p is m_1 . Now if

$$\frac{m_2^2 - M^2 - m_1^2}{2M} < m_1,$$

then the integration of the Dirac-delta function would give zero which is ensured by the step function.

2.4 Explicit computation of C -type triangle diagrams

$$M = \text{sgn}(k_1^0) \sqrt{-k_1^2} \quad (2.31)$$

So we get the an exact finite answer for C_{PPR} for time-like k_1 which is given by

$$C_{PPR} \Big|_{\text{time-like } k_1} = \frac{-2\pi i}{(4\pi)^2 \sqrt{-\Sigma^2}} \Theta \left(\frac{-k_1^2 - m_1^2 + m_2^2}{2 \text{sgn}(k_1^0) \sqrt{-k_1^2}} \right) \Theta \left(\frac{k_1^2 - m_1^2 + m_2^2}{2 \text{sgn}(k_1^0) \sqrt{-k_1^2}} - m_1 \right) \\ \times \tanh^{-1} \left(\frac{(k_1 \cdot k_3)(k_1^2 - m_1^2 + m_2^2) + k_1^2(k_3^2 - m_1^2 + m_3^2 - i\varepsilon)}{\sqrt{-\Sigma^2} \{ (k_1^2 - m_1^2 + m_2^2)^2 + 4k_1^2 m_1^2 \}} \right) \quad (2.32)$$

where we have already defined Σ^2 in last section, which is given by

$$\Sigma \equiv k_1^2 k_3^2 - k_1 \cdot k_3 \quad (2.33)$$

When we set $m_1 = m_2$, the product of the two step functions in the above result looks like

$$\Theta \left(-\frac{1}{2} \text{sgn}(k_1^0) \sqrt{-k_1^2} - m_1 \right) \Theta \left(\frac{1}{2} \text{sgn}(k_1^0) \sqrt{-k_1^2} \right) = \Theta(\text{-ve no.}) \Theta(k_1^0) \quad (2.34)$$

which is clearly zero. Thus the integral vanishes in this case.

2.4.3 TRIPLE CUT C-TYPE DIAGRAM

Here we will calculate C_{PPP} from the list of all possible triple cut C -type diagrams. The diagram is shown in figure (2.4).

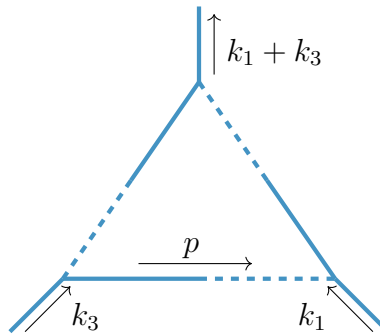


Figure 2.4: C_{PPP}

2 Open ϕ^4 scalar SK effective theory

The integral expression for C_{PPP} is the following.

$$\begin{aligned} C_{PPP}(k_1, k_2, k_3) &= \int \frac{d^4 p}{(2\pi)^4} (2\pi)\delta_+(p^2 + m_1^2)(2\pi)\delta_+((p + k_1)^2 + m_2^2)(2\pi)\delta_+((p - k_3)^2 + m_3^2) \\ &= \frac{1}{2\pi} \int d^4 p \delta_+(p^2 + m_1^2)\delta_+((p + k_1)^2 + m_2^2)\delta_+((p - k_3)^2 + m_3^2) \end{aligned} \quad (2.35)$$

We assume that k_1 and k_3 are linearly independent. Here we consider two possible cases

1. k_1, k_3 determine a null plane i.e. their span is devoid of any time-like vector
2. k_1, k_3 do not determine a null plane i.e. their span contains a time-like vector

k_1, k_3 LIE ON A NULL PLANE

In this case we can assume both k_1, k_3 to be space-like. Let us work in the frame where $k_1^0 = 0$. Further, like earlier, let

$$\begin{aligned} k_1^\mu &= (0, 0, 0, |\mathbf{k}_1|) \\ k_3^\mu &= (k_3^0, |\mathbf{k}_3| \sin \theta_0, 0, |\mathbf{k}_3| \cos \theta_0) \end{aligned} \quad (2.36)$$

We integrate p^0 , followed by θ as in the double cut case. We end up with

$$\frac{2\pi}{(4\pi)^2 |\mathbf{k}_1|} \int \frac{|\mathbf{p}| d|\mathbf{p}| d\phi}{\omega_p} \Theta \left(|\mathbf{p}| - \frac{|k_1^2 + m_2^2 - m_1^2|}{2|\mathbf{k}_1|} \right) \delta((p - k_3)^2 + m_3^2) \Big|_{p^0 = \omega_p, \cos \theta = \frac{m_1^2 - m_2^2 - k_1^2}{2|\mathbf{k}_1||\mathbf{p}|}} \quad (2.37)$$

Now, if we look at the large $|\mathbf{q}|$ sector of the above integral, we find

$$\begin{aligned} \cos \theta &\approx 0 \\ \omega_p &\approx |\mathbf{p}| \\ \delta((p - k_3)^2 + m_3^2) \Big|_{p^0 = \omega_p, \cos \theta = \frac{m_1^2 - m_2^2 - k_1^2}{2|\mathbf{k}_1||\mathbf{p}|}} &\approx \Theta(|\mathbf{k}_3| \sin \theta_0 - |k_3^0|) \frac{\delta \left(\cos \phi - \frac{k_3^0}{\sin \theta_0 |\mathbf{k}_3|} \right)}{2|\mathbf{p}| |\mathbf{k}_3| \sin \theta_0} \end{aligned} \quad (2.38)$$

The ϕ integral evaluates to

$$\int_0^{2\pi} d\phi \delta \left(\cos \phi - \frac{k_3^0}{\sin \theta_0 |\mathbf{k}_3|} \right) = \frac{2|\mathbf{k}_3| \sin \theta_0}{\sqrt{|\mathbf{k}_3|^2 \sin^2 \theta_0 - (k_3^0)^2}} \quad (2.39)$$

So the entire integral in the large momentum sector takes the form

$$\frac{2\pi \Theta(|\mathbf{k}_3| \sin \theta_0 - |k_3^0|)}{(4\pi)^2 |\mathbf{k}_1| \sqrt{|\mathbf{k}_3|^2 \sin^2 \theta_0 - (k_3^0)^2}} \int_{m_1}^\Lambda d|\mathbf{p}| \left(\frac{1}{|\mathbf{p}|} + \mathcal{O} \left(\frac{1}{|\mathbf{p}|^2} \right) \right) \quad (2.40)$$

In the Lorentz covariant form the above result looks like

$$\operatorname{div}(C_{PPP}) \Big|_{k_1, k_3 \text{ lie on a null plane}} = \frac{2\pi}{(4\pi)^2 \Sigma} \log(\Lambda) \quad (2.41)$$

where $\Sigma^2 \equiv k_1^2 k_3^2 - (k_1 \cdot k_3)^2$ following our convention

We will now show that the condition $k_1^2 k_3^2 > (k_1 \cdot k_3)^2$ is equivalent to the statement that the span of k_1, k_3 doesn't contain any time-like vector.

Let $\alpha k_1 + \beta k_3$ lie in the span of k_1, k_3 .

$$(\alpha k_1 + \beta k_3)^2 = \alpha^2 k_1^2 + \beta^2 k_3^2 + 2\alpha\beta k_1 \cdot k_3 \quad (2.42)$$

Now,

$$k_1^2 k_3^2 > (k_1 \cdot k_3)^2 \implies |k_1 \cdot k_3| < \sqrt{k_1^2 k_3^2} \implies (\alpha k_1 + \beta k_3)^2 > \left(\alpha \sqrt{k_1^2} - \beta \sqrt{k_3^2} \right)^2 \geq 0 \quad \forall \alpha, \beta \quad (2.43)$$

while,

$$k_1^2 k_3^2 < (k_1 \cdot k_3)^2 \implies |k_1 \cdot k_3| > \sqrt{k_1^2 k_3^2} \implies (\alpha k_1 + \beta k_3)^2 < \left(\alpha \sqrt{k_1^2} - \beta \sqrt{k_3^2} \right)^2 \quad (2.44)$$

So when $\alpha = \frac{\beta \sqrt{k_3^2}}{\sqrt{k_1^2}}$, $(\alpha k_1 + \beta k_3)^2 < 0$ and thus we would have a time-like vector in the linear span of k_1, k_3 .

k_1, k_3 DO NOT LIE ON A NULL PLANE

Then there exists a time-like vector in the linear span of k_1, k_3 . We will perform the integral in the rest frame of that time-like vector.

Let $\alpha k_1 + \beta k_3$ be a time-like vector. We will assume $\alpha \neq 0$. Then in the rest frame of this vector, $k_3 = -\frac{\beta}{\alpha} k_1$. After performing the p^0 integral we have

$$\frac{1}{4\pi} \int \frac{d^3 p}{\omega_p} \delta_+((p + k_1)^2 + m_2^2) \Big|_{p^0 = \omega_p} \delta_+((p - k_3)^2 + m_3^2) \Big|_{p^0 = \omega_p} \quad (2.45)$$

2 Open ϕ^4 scalar SK effective theory

Let k_1 be along the \hat{z} direction and the angle between p and k_1 be θ . Now the delta functions can be written as

$$\begin{aligned} & \delta_+((p+k_1)^2+m_2^2)|_{p^0=\omega_p} \\ &= \Theta(\omega_p+k_1^0)\Theta\left(1-\frac{|2\omega_p k_1^0+m_1^2-m_2^2-k_1^2|}{2|p||k_1|}\right)\frac{\delta\left(\cos\theta-\frac{2\omega_p k_1^0+m_1^2-m_2^2-k_1^2}{2|p||k_1|}\right)}{2|p||k_1|} \end{aligned} \quad (2.46)$$

and

$$\begin{aligned} & \delta_+((p-k_1)^2+m_3^2)\Big|_{p^0=\omega_p, \cos\theta=\frac{2\omega_p k_1^0+m_1^2-m_2^2-k_1^2}{2|p||k_1|}} \\ &= \Theta(\omega_p-m_1)\Theta(\omega_p-k_3^0)\frac{\delta\left(\omega_p+\frac{k_3^2+m_3^2-m_1^2+\frac{\beta}{\alpha}(m_1^2-m_2^2-k_1^2)}{2(k_3^0+\frac{\beta}{\alpha}k_1^0)}\right)}{2\left|k_3^0+\frac{\beta}{\alpha}k_1^0\right|} \end{aligned} \quad (2.47)$$

We perform the θ and ω_p integrals using the two delta functions. The ϕ integral just gives an extra 2π factor.

$$\frac{2\pi\Theta_{\text{overall}}}{16\pi|k_1|\left|k_3^0+\frac{\beta}{\alpha}k_1^0\right|} = \frac{\Theta_{\text{overall}}}{8|k_1|\left|k_3^0+\frac{\beta}{\alpha}k_1^0\right|} \quad (2.48)$$

where

$$\begin{aligned} \Theta_{\text{overall}} &= \left[\Theta(\omega_p+k_1^0)\Theta(\omega_p-m_1) \right. \\ & \quad \left. \times \Theta(\omega_p-k_3^0)\Theta\left(1-\frac{|2\omega_p k_1^0+m_1^2-m_2^2-k_1^2|}{2|p||k_1|}\right) \right] \Big|_{\omega_p=-\frac{k_3^2+m_3^2-m_1^2+\frac{\beta}{\alpha}(m_1^2-m_2^2-k_1^2)}{2(k_3^0+\frac{\beta}{\alpha}k_1^0)}} \end{aligned} \quad (2.49)$$

In the Lorentz covariant form the above result looks like

$$C_{PPP}\Big|_{k_1, k_3 \text{ donot lie on a null plane}} = \frac{|\alpha|\Theta_{\text{overall}}}{8\sqrt{(k_1(\alpha k_3+\beta k_1))^2-k_1^2(\alpha k_3+\beta k_1)^2}} \quad (2.50)$$

where Θ_{overall} can also be cast into Lorentz covariant form after making the substitutions

$$\begin{aligned} k_3^0 &= -\text{sgn}(\alpha k_3^0+\beta k_1^0)\frac{k_3(\alpha k_3+\beta k_1)}{\sqrt{-(\alpha k_3+\beta k_1)^2}} \\ k_1^0 &= -\text{sgn}(\alpha k_3^0+\beta k_1^0)\frac{k_1(\alpha k_3+\beta k_1)}{\sqrt{-(\alpha k_3+\beta k_1)^2}} \\ |k_1| &= \frac{\sqrt{(k_1(\alpha k_3+\beta k_1))^2-k_1^2(\alpha k_3+\beta k_1)^2}}{\sqrt{-(\alpha k_3+\beta k_1)^2}} \end{aligned} \quad (2.51)$$

3 NON-LOCAL DIVERGENCE AT ONE-LOOP IN OPEN SCALAR FIELD THEORIES

In this chapter we will derive the form of all possible non-local divergence structures that arise at one loop in open scalar field theories. It won't come as too much surprise that the cut-free diagrams at one loop don't ever have non-local divergence. We nevertheless compute it's explicit form of divergence and comment on why that is the case. The single cut diagrams do show non-local divergence as do the multi-cut diagrams, albeit in a particular regime of the choice of external momenta. Note that we will eventually restrict our analysis to the leading divergence structure in all cases. In the critical log-divergent case, the leading divergence is all that is there.

Consider a generic one-loop cut diagram made out of the P and R type propagators as shown in (3.1). The dotted internal lines are for the P propagators while the solid internal lines are for the R propagator. We will work in D spacetime dimensions with N external legs and N_c cuts such that $N_c \leq D, N$. Since all the P 's are cyclically successive and so are all the R 's, we call this diagram $P^{N_c} R^{N-N_c}$.

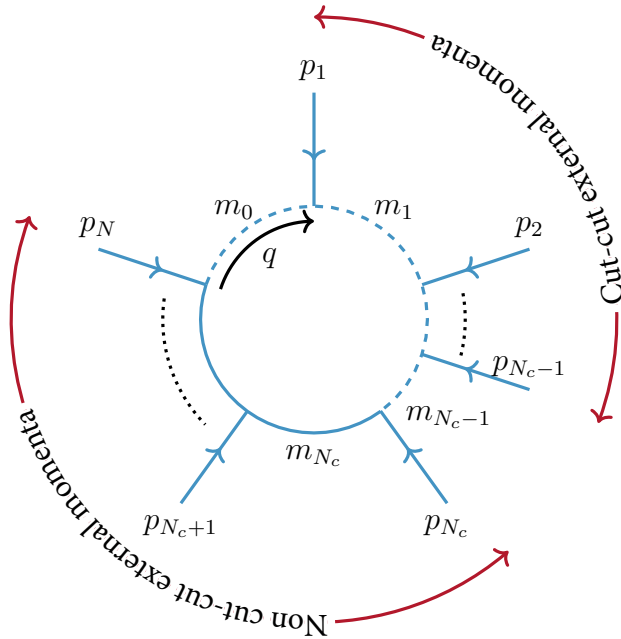


Figure 3.1: A generic one-loop cut diagram with N external legs and N_c cut propagators

3 Non-local divergence at one-loop in open scalar field theories

We adopt a simple convention for labelling various parts of the diagram. We follow a clockwise labelling convention for the vertices starting with 1 at the north pole. Let p_i denote the external momenta entering the i^{th} vertex. Let m_0 be the mass of the N^{th} propagator and m_i the mass of the i^{th} propagator for $1 \leq i \leq N-1$. Further, we fix the N^{th} propagator (cut) of mass m_0 as our reference and note that the external momentum entering between the reference cut propagator and the i^{th} propagator is

$$k_i = \sum_{j=1}^i p_j, \quad 1 \leq i \leq N-1 \quad (3.1)$$

The set $\{k_i\}$ contains the same kinematical data as the set $\{p_i\}$, but the former directly enters into the loop integral expression through the propagators of the internal lines.

It is useful to group the external momenta p_i 's into two classes:

1. Cut-cut: These are the external momenta that enter between pairs of cut propagators (both P or both M). In figure (3.1), the set of cut-cut momenta is $\{p_1, p_2, \dots, p_{N_c-1}\}$
2. Non cut-cut: These are the external momenta that either enter between a pair of usual Feynman propagators (either R or L) or between a cut and a Feynman propagator (between P/M and L/R). In figure (3.1), the set of non cut-cut momenta is $\{p_{N_c}, p_{N_c+1}, \dots, p_N\}$.

Note that in (3.1), we have taken all the cut propagators to be cyclically successive, but in general they can come in any order. In any case, we can always draw an equivalent diagram of the form in figure (3.1) as we shall show below.

In (3.2), we can see that a hexagon diagram with three non-successive cut propagators is equivalent to another hexagon diagram with successive cut propagators.

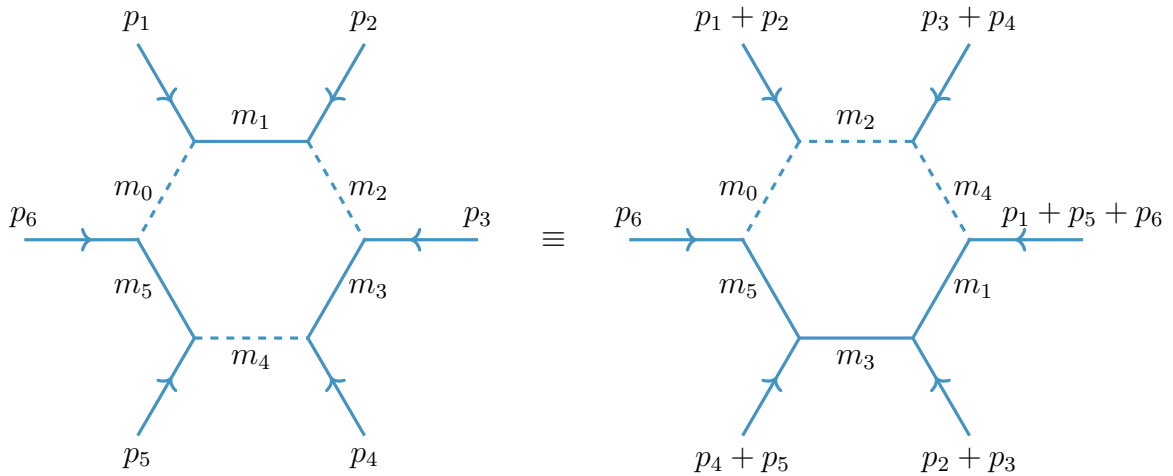


Figure 3.2: A hexagon diagram with non-successive cut propagators is equivalent to one with successive cut propagators

With this basic discussion, we are ready to compute the generic one-loop cut integral corresponding to the diagram $P^{N_c} R^{N-N_c}$ in (3.1)

$$(-i)^{N-N_c} \int \frac{d^D q}{(2\pi)^D} \frac{(2\pi)\delta_+(q^2 + m_0^2) \prod_{i=1}^{N_c-1} (2\pi)\delta_+((q + k_i)^2 + m_i^2)}{\prod_{i=N_c}^{N-1} [(q + k_i)^2 + m_i^2 - i\epsilon]} \quad (3.2)$$

ASSUMPTIONS ON EXTERNAL MOMENTA

We make some assumptions on the choice of external momenta. As we shall see in the subsequent sections, it is only in the presence of these assumptions that the Feynman diagram not only has a non-trivial divergence structure but also the structure is universal i.e. it is independent of the masses of the internal lines.

1. The spatial part of the cut-cut momenta are linearly independent. From this it follows that the cut-cut momenta are linearly independent in the full Minkowski spacetime.
2. For each of the non cut-cut momentum, its spatial part is linearly independent with respect to the spatial part of all the cut-cut momenta.
3. The cut-cut momenta lie on a null plane. In particular, the cut-cut momenta and any linear combination of them is space-like.

We will divide our subsequent analysis into three parts with increasing generality and/or complexity. In the first part, we will review one-loop diagrams without any cut propagator (cut-free diagrams). In the second part, we will work out the integral for a generic single cut diagram. In the last part, we will explore multi-cut diagrams.

3.1 CUT-FREE

Although these diagrams are the simplest and most well-known class of one-loop diagrams, we will still write down a general expression for its divergence. This will help us compare its divergence structure against single or multiple cut diagrams. With $N_c = 0$, the integral in (3.2) reduces to

$$(-i)^N \int \frac{d^D q}{(2\pi)^D} \frac{1}{\prod_{i=1}^N [(q + k_i)^2 + m_i^2 - i\epsilon]} \quad (3.3)$$

such that $\sum_{i=1}^N k_i = 0$.

3 Non-local divergence at one-loop in open scalar field theories

Dressing the above integral in Feynman parameters we obtain¹

$$\frac{(-i)^N}{(2\pi)^D} \int_{\Delta^{N-1}} \prod_{i=1}^N dx_i \int \frac{d^D q}{\left(q^2 + 2q \cdot \tilde{k}(x_i) + K(x_i)\right)^N} \quad (3.4)$$

where

$$\begin{aligned} \tilde{k}(x_i) &\equiv \sum_{i=1}^N k_i x_i \\ K(x_i) &\equiv \sum_{i=1}^N x_i (k_i^2 + m_i^2) - i\epsilon \end{aligned} \quad (3.5)$$

We now get rid of the linear term, downstairs of the integrand in (3.4) by shifting q by $\tilde{k}(x_i)$ i.e. $q \rightarrow q' = q + \tilde{k}(x_i)$:

$$\frac{(-i)^N}{(2\pi)^D} \int_{\Delta^{N-1}} \prod_{i=1}^N dx_i \int \frac{d^D q}{\left(q^2 + K'(x_i)\right)^N} \quad (3.6)$$

where

$$K'(x_i) = K(x_i) - \tilde{k}^2(x_i) \quad (3.7)$$

We can now perform a Wick rotation to Euclideanize the above integral

$$\frac{(-i)^{N+1}}{(2\pi)^D} \int_{\Delta^{N-1}} \prod_{i=1}^N dx_i \int \frac{d^D q_E}{\left(q_E^2 + K'(x_i)\right)^N} \quad (3.8)$$

where q_E refers to loop momentum in Euclidean space. Next we can employ spherical coordinates to exploit the spherical symmetry and to reduce the D -dimensional Euclidean integral to just one radial direction.

$$\frac{(-i)^{N+1}}{(2\pi)^D} \int d\Omega_{D-1} \int_{\Delta^{N-1}} \prod_{i=1}^N dx_i \int \frac{d|q_E| |q_E|^{D-1}}{\left(|q_E|^2 + K'(x_i)\right)^N} \quad (3.9)$$

To check for divergent behavior we expand the integrand of the $|q_E|$ integral in $|q_E|$ and integrate in the large momentum sector

¹our notation $\int_{\Delta^{N-1}} \prod_{i=1}^N dx_i$ stands for $\int \prod_{i=1}^N dx_i \delta\left(1 - \sum_{i=1}^N x_i\right)$ and Δ^{N-1} just refers to the $(N-1)$ -simplex

$$\text{div}(R^N) \Big|_{D-2N \geq 0} = \frac{(-i)^{N+1}}{(2\pi)^D} \text{Vol}(\mathbb{S}^{D-1}) \text{Vol}(\Delta^{N-1}) \int d|\mathbf{q}_E| |\mathbf{q}_E|^{D-2N-1} \left[1 + \mathcal{O}\left(\frac{1}{|\mathbf{q}_E|}\right) \right] \quad (3.10)$$

From the above formula, we can note the following points

1. The leading divergence of cut-free one-loop diagrams is always independent of external momenta. This is because of the spherical symmetry of the integral.
2. The subleading divergences may in general have at most polynomial dependencies in the external momenta. Thus the complete divergence is local.
3. The degree of divergence is $D - 2N$. So whenever $D = 2N$, we have the critical case of logarithmic divergence. In that situation, there are no subleading divergences and hence the above expression gives the full answer.

Special Case: Log Divergence

Since $D = 2N$ for log divergence, they are only possible in even number of dimensions. With $D = 2N$ in (3.10), the integral reduces to

$$\text{div}(R^{\frac{D}{2}}) = \frac{(-i)^{\frac{D}{2}+1}}{(2\pi)^D} \text{Vol}(\mathbb{S}^{D-1}) \text{Vol}\left(\Delta^{\frac{D}{2}-1}\right) \log(\Lambda) \quad (3.11)$$

3.2 SINGLE CUT

The story gets interesting from this section onwards. We will encounter non-local divergences under certain conditions on and D, N .

Here, $N_c = 1$ and the integral (3.2) reduces to just

$$(-i)^{N-1} \int \frac{d^D q}{(2\pi)^D} \times \frac{2\pi \delta_+(q^2 + m_0^2)}{\prod_{i=1}^{N-1} [(q + k_i)^2 + m_i^2 - i\epsilon]} \quad (3.12)$$

We just use the fact $\delta_+(q^2 + m_0^2) = \frac{\delta(q^0 - \omega_q)}{2\omega_q}$ where $\omega_q = \sqrt{|\mathbf{q}|^2 + m_0^2}$ to perform the q^0 integral.

$$\frac{(-i)^{N-1}}{2(2\pi)^{D-1}} \int \frac{d^{D-1} q}{\omega_q \prod_{i=1}^{N-1} [-2\omega_q k_i^0 + 2\mathbf{q} \cdot \mathbf{k}_i + k_i^2 + m_i^2 - m_0^2 - i\epsilon]} \quad (3.13)$$

3 Non-local divergence at one-loop in open scalar field theories

We look at the large momentum behavior of the above integral by expanding the integrand in $\frac{1}{|q|}$

$$\frac{(-i)^{N-1}}{2^N (2\pi)^{D-1}} \int \frac{d\Omega_{D-2}}{\prod_{i=1}^{N-1} (-k_i^0 + \hat{\mathbf{q}} \cdot \mathbf{k}_i)} \int d|q| |q|^{D-N-2} \left(1 + \mathcal{O}\left(\frac{1}{|q|}\right) \right) \quad (3.14)$$

We next pass to Feynman parameters and cast the $(N - 1)$ propagators as an integral over an $(N - 2)$ -simplex.

$$\frac{1}{\prod_{i=1}^{N-1} (-k_i^0 + \hat{\mathbf{q}} \cdot \mathbf{k}_i)} = \int_{\Delta^{N-2}} \frac{\prod_{i=1}^{N-1} dx_i}{(\hat{q} \cdot \tilde{k}(x_i))^{N-1}} \quad (3.15)$$

where

$$\begin{aligned} \hat{q} &\equiv (1, \hat{\mathbf{q}}) \\ \tilde{k}(x_i) &= \sum_{i=1}^{N-1} k_i x_i \end{aligned} \quad (3.16)$$

If we let θ be the angle between $\hat{\mathbf{q}}$ and \mathbf{k} , we can perform the angular integral as

$$\begin{aligned} \int \frac{d\Omega_{D-2}}{(\hat{q} \cdot \tilde{k})^{N-1}} &= \int d\Omega_{D-3} \int_0^\pi \frac{\sin^{D-3} \theta d\theta}{(-\tilde{k}^0 + |\mathbf{k}| \cos \theta)^{N-1}} \\ &= \text{Vol}(\mathbb{S}^{D-3}) \frac{\sqrt{\pi} \Gamma\left(\frac{D-2}{2}\right) {}_2F_1\left(\frac{N-1}{2}, \frac{N}{2}, \frac{D-1}{2}, \frac{|\mathbf{k}|^2}{(\tilde{k}^0)^2}\right)}{(-\tilde{k}^0)^{N-1} \Gamma\left(\frac{D-1}{2}\right)} \\ &= (-1)^{N-1} \text{Vol}(\mathbb{S}^{D-2}) \frac{{}_2F_1\left(\frac{N-1}{2}, \frac{N}{2}, \frac{D-1}{2}, \frac{|\mathbf{k}|^2}{(\tilde{k}^0)^2}\right)}{(\tilde{k}^0)^{N-1}} \end{aligned} \quad (3.17)$$

Thus the divergent portion of the integral for $D - N \geq 1$ looks like

$$\text{div}(PR^{N-1}) \Big|_{D-N \geq 1} = \frac{i^{N-1} \text{Vol}(\mathbb{S}^{D-2})}{2^N (2\pi)^{D-1}} \int_{\Delta^{N-2}} \prod_{i=1}^{N-1} dx_i \frac{{}_2F_1\left(\frac{N-1}{2}, \frac{N}{2}, \frac{D-1}{2}, \frac{|\mathbf{k}|^2}{(\tilde{k}^0)^2}\right)}{(\tilde{k}^0)^{N-1}} \times \int d|q| |q|^{D-N-2} \left(1 + \mathcal{O}\left(\frac{1}{|q|}\right) \right) \quad (3.18)$$

From the above expression, we can conclude the following

1. The above expression gives us information about the universal leading divergence structure provided $D - N - 1 \geq 0$. The subleading divergences (if present) will in general depend on details of the theory like masses of the propagators.
2. The integral has degree of divergence $D - N - 1$. $D - N = 1$ is the critical case of logarithmic divergence. In that case there are no subleading divergences and hence the above result is exact.

Special case: Non-local log divergence

We will now specialize to the case of log divergence i.e. $D - N = 1$. Then the expression (3.18) simplifies dramatically. Firstly, the Gauss hypergeometric function simplifies as

$$\begin{aligned}
{}_2F_1\left(\frac{N-1}{2}, \frac{N}{2}; \frac{D-1}{2}; \frac{|\mathbf{k}|^2}{(\tilde{k}^0)^2}\right) &= {}_2F_1\left(\frac{D-2}{2}, \frac{D-1}{2}; \frac{D-1}{2}; \frac{|\mathbf{k}|^2}{(\tilde{k}^0)^2}\right) \\
&= \frac{1}{\left(1 - \frac{|\mathbf{k}|^2}{(\tilde{k}^0)^2}\right)^{\frac{D-2}{2}}}
\end{aligned} \tag{3.19}$$

The Feynman parameter integral over the $(N-2)$ -simplex then looks like

$$\int_{\Delta^{D-3}} \prod_{i=1}^{D-2} dx_i \frac{\text{sgn}^{D-2}(\tilde{k}^0)}{(-\tilde{k}^2)^{\frac{D-2}{2}}} \tag{3.20}$$

and hence the simplified result takes the form

$$\text{div}(PR^{D-2}) = \frac{i^{D-2} \text{Vol}(\mathbb{S}^{D-2})}{2^{D-1} (2\pi)^{D-1}} \int_{\Delta^{D-3}} \prod_{i=1}^{D-2} dx_i \frac{\text{sgn}^{D-2}(\tilde{k}^0)}{(-\tilde{k}^2)^{\frac{D-2}{2}}} \log(\Lambda) \tag{3.21}$$

3.3 MULTIPLE CUT

We will now determine the divergent structures arising in multi-cut one-loop diagrams. This is a big step up from the single-cut case and we employ some neat tricks to extract the divergence.

As mentioned earlier, we will assume the cut-cut momenta to be spatially linearly independent, space-like and further lying on a null plane. The non cut-cut momenta have rather mild restriction that each must be spatially linearly independent wrt all the cut-cut momenta.

From the get go, we will focus on the large $|\mathbf{q}|$ sector of the cut integral and check for divergent behavior.

3 Non-local divergence at one-loop in open scalar field theories

Let us set up a spherical polar coordinate system where the orthonormal basis is nothing but the Gram-Schmidt basis for the set of spatial part of all the external momenta together with the spatial part of the loop momentum.²

$$\begin{aligned}
\mathbf{k}_1 &= |\mathbf{k}_1| \hat{e}_1 \\
\mathbf{k}_2 &= |\mathbf{k}_2| (\cos \alpha_{21} \hat{e}_1 + \sin \alpha_{21} \hat{e}_2) \\
\mathbf{k}_3 &= |\mathbf{k}_3| (\cos \alpha_{31} \hat{e}_1 + \sin \alpha_{31} \cos \alpha_{32} \hat{e}_2 + \sin \alpha_{31} \sin \alpha_{32} \hat{e}_3) \\
&\vdots \\
\mathbf{k}_{N-1} &= |\mathbf{k}_{N-1}| (\cos \alpha_{(N-1)1} \hat{e}_1 + \sin \alpha_{(N-1)1} \cos \alpha_{(N-1)2} \hat{e}_2 + \dots \\
&\quad + \sin \alpha_{(N-1)1} \dots \sin \alpha_{(N-1)(N-2)} \hat{e}_{N-1})
\end{aligned} \tag{3.22}$$

and

$$\begin{aligned}
\mathbf{q} &= |\mathbf{q}| (\cos \theta_1 \hat{e}_1 + \sin \theta_1 \cos \theta_2 \hat{e}_2 + \sin \theta_1 \sin \theta_2 \cos \theta_3 \hat{e}_3 + \dots \\
&\quad + \sin \theta_1 \sin \theta_2 \dots \cos \theta_{D-2} \hat{e}_{D-2} + \sin \theta_1 \sin \theta_2 \dots \sin \theta_{D-2} \hat{e}_{D-1})
\end{aligned} \tag{3.23}$$

The delta functions in the large momenta sector after integrating them out one by one look like

$$\begin{aligned}
\delta_+(q^2 + m_0^2) &= \frac{\delta\left(q^0 - |\mathbf{q}| + \mathcal{O}\left(\frac{1}{|\mathbf{q}|}\right)\right)}{2\left(|\mathbf{q}| + \mathcal{O}\left(\frac{1}{|\mathbf{q}|}\right)\right)} \\
\delta_+((q + k_1)^2 + m_1^2)|_{q^0} &= \frac{\delta\left(\cos \theta_1 - \frac{k_1^0}{|\mathbf{k}_1|} + \mathcal{O}\left(\frac{1}{|\mathbf{q}|}\right)\right)}{2|\mathbf{k}_1||\mathbf{q}|} \\
\delta_+((q + k_2)^2 + m_2^2)|_{q^0, \theta_1} &= \frac{\delta\left(\cos \theta_2 - \frac{k_2^0}{|\mathbf{k}_2|} - \frac{\cos \alpha_{21} \cos \theta_1}{\sin \alpha_{21} \sin \theta_1} + \mathcal{O}\left(\frac{1}{|\mathbf{q}|}\right)\right)}{2|\mathbf{k}_2||\mathbf{q}| \sin \alpha_{21} \sin \theta_1} \\
\delta_+((q + k_3)^2 + m_3^2)|_{q^0, \theta_1, \theta_2} &= \frac{\delta\left(\cos \theta_3 - \frac{k_3^0}{|\mathbf{k}_3|} - \frac{\cos \alpha_{31} \cos \theta_1 - \sin \alpha_{31} \cos \alpha_{32} \sin \theta_1 \cos \theta_2}{\sin \alpha_{31} \sin \alpha_{32} \sin \theta_1 \sin \theta_2} + \mathcal{O}\left(\frac{1}{|\mathbf{q}|}\right)\right)}{2|\mathbf{k}_3||\mathbf{q}| \sin \alpha_{31} \sin \alpha_{32} \sin \theta_1 \sin \theta_2} \\
&\vdots \\
\delta_+((q + k_{N_c-1})^2 + m_{N_c-1}^2)|_{q^0, \theta_1, \theta_2, \dots, \theta_{N_c-2}} &= \frac{\delta\left(\cos \theta_{N_c-1} - \frac{k_{N_c-1}^0}{|\mathbf{k}_{N_c-1}|} - \frac{(\hat{\mathbf{q}} \cdot \hat{\mathbf{k}}_{N_c-1})_{\theta_1, \theta_2, \dots, \theta_{N_c-2}}}{\prod_{j=1}^{N_c-2} \sin \alpha_{N_c-1j} \sin \theta_j} + \mathcal{O}\left(\frac{1}{|\mathbf{q}|}\right)\right)}{2|\mathbf{k}_{N_c-1}||\mathbf{q}| \prod_{j=1}^{N_c-2} \sin \alpha_{N_c-1j} \sin \theta_j}
\end{aligned} \tag{3.24}$$

²We already know that the superficial degree of divergence is $D - N - 1$. Thus for divergent diagrams, $D - 1 \geq N > N - 1$. Hence the subspace spanned by the spatial part of $N - 1$ external momenta has a positive codimension wrt the spatial part of the D -dimensional ambient Minkowski space.

where $(\hat{\mathbf{q}} \cdot \hat{\mathbf{k}}_i)_{\theta_1, \theta_2, \dots, \theta_{i-1}}^{\parallel \text{to } \langle \mathbf{k}_1, \mathbf{k}_2, \dots, \mathbf{k}_{i-1} \rangle}$ is the component of $\hat{\mathbf{k}}_i$ along the $\hat{\mathbf{q}}$ direction in the plane fixed on imposing all the i previous onshell conditions.

The fact that, corresponding to each delta function condition, there exists some θ_i such that $\cos \theta_i$ has modulus less than one, is guaranteed by the choice of a null plane worth of space-like external cut-cut momenta.

Let us split the spatial part of the integration measure viz. $d^{D-1}q$ into three parts viz. radial, angles wrt spatial part of cut-cut external momenta and the rest.

$$\begin{aligned} d^{D-1}q &= |\mathbf{q}|^{D-2} d|\mathbf{q}| d\Omega_{D-2} = |\mathbf{q}|^{D-2} d|\mathbf{q}| \left(\prod_{i=1}^{N_c-1} \sin^{D-2-i} \theta_i d\theta_i \right) d\Omega_{D-N_c-1} \\ &= |\mathbf{q}|^{D-2} d|\mathbf{q}| \left(\prod_{i=1}^{N_c-1} \sin^{D-3-i} \theta_i d(-\cos \theta_i) \right) d\Omega_{D-N_c-1} \end{aligned} \quad (3.25)$$

Thus (3.2), after performing all the delta function integrals in the large $|\mathbf{q}|$ sector, looks like³

$$\begin{aligned} \text{div}(P^{N_c} R^{N-N_c}) \Big|_{D-N \geq 1} &= \frac{(-i)^{N-N_c}}{2^N (2\pi)^{D-N_c}} \int \frac{d\Omega_{D-N_c-1}}{\prod_{i=N_c}^{N-1} \hat{\mathbf{q}} \cdot \mathbf{k}_i \Big|_{\text{onshell cond.}}} \times \\ &\int d|\mathbf{q}| \left(\prod_{i=1}^{N_c-1} \frac{\sin^{D-3-i} \theta_i}{|\mathbf{k}_i| \prod_{j=1}^{i-1} \sin \alpha_{ij} \sin \theta_j} \right) \Big|_{\text{onshell cond.}} |\mathbf{q}|^{D-N-2} \left[1 + \mathcal{O}\left(\frac{1}{|\mathbf{q}|}\right) \right] \end{aligned} \quad (3.26)$$

The angular factor can be simplified using the following three facts:

1.

$$\begin{aligned} &\prod_{i=1}^{N_c-1} \frac{\sin^{N_c-2-i} \theta_i}{|\mathbf{k}_i| \prod_{j=1}^{i-1} \sin \alpha_{ij} \sin \theta_j} \Big|_{\text{onshell cond.}} \\ &= \frac{\sin^{N_c-3} \theta_1}{|\mathbf{k}_1|} \times \frac{\sin^{N_c-4} \theta_2}{|\mathbf{k}_2| \sin \alpha_{21} \sin \theta_1} \times \frac{\sin^{N_c-5} \theta_3}{|\mathbf{k}_3| \sin \alpha_{31} \sin \alpha_{32} \sin \theta_1 \sin \theta_2} \times \dots \Big|_{\text{onshell cond.}} \\ &= \frac{1}{|\mathbf{k}_1| \sin \theta_1} \times \frac{1}{|\mathbf{k}_2| \sin \alpha_{21} \sin \theta_2} \times \frac{1}{|\mathbf{k}_3| \sin \alpha_{31} \sin \alpha_{32} \sin \theta_3} \times \dots \Big|_{\text{onshell cond.}} \end{aligned}$$

³An important point to note is that if $N_c = D - 1$, then the delta functions will eat up all the angular variables including the last angle θ_{D-2} , which has $[0, 2\pi)$ domain unlike the other angles with domain $[0, \pi)$. In such a situation, the delta function in the last angle will have two zeros and hence the overall result should be multiplied with 2 to account for the extra zero.

3 Non-local divergence at one-loop in open scalar field theories

$$= \frac{1}{\left(\prod_{i=1}^{N_c-1} |\mathbf{k}_i| \sin \theta_i \right) \Big|_{\text{onshell cond.}} \left(\prod_{\substack{i,j \in \{1,2,\dots,N_c-1\} \\ i>j}} \sin \alpha_{ij} \right)} \quad (3.27)$$

Now to proceed further, we make the observation that the factor in the denominator above is nothing but the volume of the parallelotope bounded by $\mathbf{k}_1, \mathbf{k}_2, \dots, \mathbf{k}_{N_c-1}$ and $\hat{\mathbf{q}}$. Thus,

$$\text{Vol}(\{\mathbf{k}_i\}, \hat{\mathbf{q}}) = \left(\prod_{i=1}^{M-1} \mathbf{k}_i \cdot \hat{\mathbf{e}}_i \right) \times |\hat{\mathbf{q}}^\perp| = \left(\prod_{i=1}^{N_c-1} |\mathbf{k}_i| \sin \theta_i \right) \left(\prod_{\substack{i,j \in \{1,2,\dots,N_c-1\} \\ i>j}} \sin \alpha_{ij} \right) \quad (3.28)$$

We can now use the Gram determinant formula to calculate this volume

$$\begin{aligned} & \text{Vol}(\{\mathbf{k}_i\}, \hat{\mathbf{q}})^2 \\ &= \begin{vmatrix} \hat{\mathbf{q}} \cdot \hat{\mathbf{q}} & \hat{\mathbf{q}} \cdot \mathbf{k}_1 & \cdots & \hat{\mathbf{q}} \cdot \mathbf{k}_{N_c-1} \\ \mathbf{k}_1 \cdot \hat{\mathbf{q}} & \mathbf{k}_1 \cdot \mathbf{k}_1 & \cdots & \mathbf{k}_1 \cdot \mathbf{k}_{N_c-1} \\ \vdots & \vdots & \ddots & \vdots \\ \mathbf{k}_{N_c-1} \cdot \hat{\mathbf{q}} & \mathbf{k}_{N_c-1} \cdot \mathbf{k}_1 & \cdots & \mathbf{k}_{N_c-1} \cdot \mathbf{k}_{N_c-1} \end{vmatrix} \\ &= \begin{vmatrix} 1 & k_1^0 & \cdots & k_{N_c-1}^0 \\ k_1^0 & \mathbf{k}_1 \cdot \mathbf{k}_1 & \cdots & \mathbf{k}_1 \cdot \mathbf{k}_{N_c-1} \\ \vdots & \vdots & \ddots & \vdots \\ k_{N_c-1}^0 & \mathbf{k}_{N_c-1} \cdot \mathbf{k}_1 & \cdots & \mathbf{k}_{N_c-1} \cdot \mathbf{k}_{N_c-1} \end{vmatrix} + \mathcal{O}\left(\frac{1}{|\mathbf{q}|}\right) \quad (\because \hat{\mathbf{q}} \cdot \mathbf{k}_i = k_i^0 + \mathcal{O}\left(\frac{1}{|\mathbf{q}|}\right) \forall i \text{ by onshell cond.}) \\ &= \det \left(\begin{pmatrix} \mathbf{k}_1 \cdot \mathbf{k}_1 & \cdots & \mathbf{k}_1 \cdot \mathbf{k}_{N_c-1} \\ \vdots & \ddots & \vdots \\ \mathbf{k}_{N_c-1} \cdot \mathbf{k}_1 & \cdots & \mathbf{k}_{N_c-1} \cdot \mathbf{k}_{N_c-1} \end{pmatrix} - \begin{pmatrix} k_1^0 k_1^0 & \cdots & k_1^0 k_{N_c-1}^0 \\ \vdots & \ddots & \vdots \\ k_{N_c-1}^0 k_1^0 & \cdots & k_{N_c-1}^0 k_{N_c-1}^0 \end{pmatrix} \right) + \mathcal{O}\left(\frac{1}{|\mathbf{q}|}\right) \\ & \quad \left(\because \det \begin{pmatrix} \mathbb{I} & B \\ C & D \end{pmatrix} = \det(D - CB) \right) \\ &= \begin{vmatrix} k_1 \cdot k_1 & k_1 \cdot k_2 & \cdots & k_1 \cdot k_{N_c-1} \\ k_2 \cdot k_1 & k_2 \cdot k_2 & \cdots & k_2 \cdot k_{N_c-1} \\ \vdots & \vdots & \ddots & \vdots \\ k_{N_c-1} \cdot k_1 & k_{N_c-1} \cdot k_2 & \cdots & k_{N_c-1} \cdot k_{N_c-1} \end{vmatrix} \left(\equiv \Sigma_{cut}^2 \right) + \mathcal{O}\left(\frac{1}{|\mathbf{q}|}\right) \quad (3.29) \end{aligned}$$

where Σ_{cut}^2 is the Gram determinant of the cut-cut momenta and represents the square of the volume of the parallelotope (sitting inside a null plane) bounded by them. Further

the fact that the cut-cut momenta are linearly independent and determine a null plane is equivalent to the condition that $\Sigma_{cut}^2 > 0$.

This means that the onshell conditions force

$$\text{Vol}(\{\mathbf{k}_i\}_{\text{cut-cut}}, \hat{\mathbf{q}}|_{\text{onshell cond.}}) = \Sigma_{cut} + \mathcal{O}\left(\frac{1}{|\mathbf{q}|}\right) \quad (3.30)$$

For example, when the number of cuts is 2,3 or 4, Σ_{cut} looks like

- $N_c = 2 : \Sigma_{cut} = \sqrt{k_1^2}$
- $N_c = 3 : \Sigma_{cut} = \sqrt{k_1^2 k_2^2 - (k_1 k_2)^2}$
- $N_c = 4 : \Sigma_{cut} = \sqrt{k_1^2 k_2^2 k_3^2 - k_1^2 (k_2 k_3)^2 - k_2^2 (k_1 k_3)^2 - k_3^2 (k_1 k_2)^2 + 2(k_1 k_2)(k_2 k_3)(k_1 k_3)}$

2. Let $\Sigma_{cut}^{\text{space}}$ represent the volume of the parallelotope bounded by spatial part of the cut-cut momenta. This is also given in terms of square root of a Gram determinant.

$$\Sigma_{cut}^{\text{space}} \equiv \left(\prod_{i=1}^{N_c-1} |\mathbf{k}_i| \right) \left(\prod_{\substack{i,j \in \{1,2,\dots,N_c-1\} \\ i > j}} \sin \alpha_{ij} \right) = \sqrt{\begin{vmatrix} \mathbf{k}_1 \cdot \mathbf{k}_1 & \mathbf{k}_1 \cdot \mathbf{k}_2 & \cdots & \mathbf{k}_1 \cdot \mathbf{k}_{N_c-1} \\ \mathbf{k}_2 \cdot \mathbf{k}_1 & \mathbf{k}_2 \cdot \mathbf{k}_2 & \cdots & \mathbf{k}_2 \cdot \mathbf{k}_{N_c-1} \\ \vdots & \vdots & \ddots & \vdots \\ \mathbf{k}_{N_c-1} \cdot \mathbf{k}_1 & \mathbf{k}_{N_c-1} \cdot \mathbf{k}_2 & \cdots & \mathbf{k}_{N_c-1} \cdot \mathbf{k}_{N_c-1} \end{vmatrix}} \quad (3.31)$$

3. Using (3.30) and (3.31), we have the following expression for the product of $\sin \theta_i$'s in the presence of all the onshell conditions

$$\prod_{i=1}^{N_c-1} \sin \theta_i \Big|_{\text{onshell con.}} = \frac{\Sigma_{cut}}{\Sigma_{cut}^{\text{space}}} \left(1 + \mathcal{O}\left(\frac{1}{|\mathbf{q}|}\right) \right) \quad (3.32)$$

Using the above facts we can rewrite (3.26) as

$$\text{div}(P^{N_c} R^{N-N_c}) \Big|_{D-N \geq 1} = \frac{(-i)^{N-N_c}}{2^N (2\pi)^{D-N_c}} \frac{\Sigma_{cut}^{D-N_c-2}}{(\Sigma_{cut}^{\text{space}})^{D-N_c-1}} \int \frac{d\Omega_{D-N_c-1}}{\prod_{i=N_c}^{N-1} \hat{\mathbf{q}} \cdot \mathbf{k}_i \Big|_{\text{onshell cond.}}} \times \int d|\mathbf{q}| |\mathbf{q}|^{D-N-2} \left[1 + \mathcal{O}\left(\frac{1}{|\mathbf{q}|}\right) \right] \quad (3.33)$$

From the previous formula we make the following important observations:

1. If $N_c = D$, then there will be no integration to perform, and hence the result will always be finite. This is simply because the delta functions of the loop integral eat up all the components of the loop momentum.

3 Non-local divergence at one-loop in open scalar field theories

2. If $N_c < D$, we have three cases

- a) If $D - N < 1$, there is no divergence.
- b) If $D - N = 1$, the divergence is logarithmic and there are no subleading divergences. Hence the above result is exact.
- c) If $D - N > 1$, the above result gives us the form of the leading universal divergence only. The subleading divergences will in general depend on the masses of the various propagators.

3. If we restrict to the special case $N_c = D - 1$, there are no leftover angular integrals to perform. The integral in (3.33) thus reduces to⁴

$$\text{div}(P^{D-1}R^{N-D+1}) \Big|_{D-N \geq 1} = \frac{2(-i)^{N-D+1}}{2^N 2\pi} \frac{1}{\Sigma_{cut} \left(\prod_{i=D-1}^{N-1} \hat{q} \cdot k_i \right) \Big|_{\text{onshell cond.}}} \times \int d|\mathbf{q}| |\mathbf{q}|^{D-N-2} \left[1 + \mathcal{O}\left(\frac{1}{|\mathbf{q}|}\right) \right] \quad (3.34)$$

Further, if $N_c = N = D - 1$, which is the case where all the propagators are cut-propagators, we have logarithmic divergence with a very simple form

$$\text{div}(P^{D-1}) = \frac{1}{2^{D-1}\pi} \frac{1}{\Sigma_{cut}} \log(\Lambda) \quad (3.35)$$

where Λ is a cutoff

Its very easy to see from here that for C_{PPP} in 4 dimensions, we get the answer as $\frac{\log(\Lambda)}{8\pi\sqrt{k_1^2 k_2^2 - (k_1 \cdot k_2)^2}}$ which matches with our explicit calculation done in the previous section of the appendix.

We now pick up from (3.33), turning our attention to the evaluation of the angular integral for $N_c < D$. We can make use of Feynman parameters to first make the integrand a function of one angle only out of the $D - N_c - 1$ of them. Let θ be the angle between $\hat{\mathbf{q}}$ and the part of the convex hull of spatial part of the non cut-cut external momenta, $\sum_{i=1}^{N-N_c} x_i \mathbf{k}_{N_c+i-1}$, lying perpendicular to the spatial region spanned by the cut-cut external momenta. Then,

$$\int \frac{d\Omega_{D-N_c-1}}{\prod_{i=N_c}^{N-1} \hat{q} \cdot k_i} = \int d\Omega_{D-N_c-2} \int_{\Delta^{N-N_c-1}} \left(\prod_{i=1}^{N-N_c} dx_i \right) \int \frac{\sin^{D-N_c-2} \theta d\theta}{\left(\hat{\mathbf{q}} \cdot \tilde{\mathbf{k}}(x_i) \Big|_{\text{onshell cond.}} \right)^{N-N_c}} \quad (3.36)$$

⁴we have multiplied the usual answer by 2 as the delta functions eat up the last angular coordinate as well, whose domain is $[0, 2\pi)$

where

$$\tilde{\mathbf{k}}(x_i) \equiv \sum_{i=1}^{N-N_c} x_i \mathbf{k}_{N_c+i-1} \quad (3.37)$$

Now we can decompose $\mathbf{k}(x_i)$ into two parts, $\mathbf{k}^{\parallel}(x_i)$ being in the span of the spatial part of cut-cut momenta and $\mathbf{k}^{\perp}(x_i)$ being the rest of $\mathbf{k}(x_i)$. Focusing on the θ integral in (3.36) we have

$$\int_0^{\pi} \frac{\sin^{D-N_c-3} \theta d(-\cos \theta)}{\left(\hat{q} \cdot \tilde{\mathbf{k}}^{\parallel}(x_i) + |\hat{\mathbf{q}}^{\perp}| |\tilde{\mathbf{k}}^{\perp}(x_i)| \cos \theta\right)^{N-N_c}} = \frac{\sqrt{\pi} \Gamma\left(\frac{D-N_c-1}{2}\right)}{\Gamma\left(\frac{D-N_c}{2}\right)} \frac{{}_2F_1\left(\frac{N-N_c}{2}, \frac{N-N_c+1}{2}; \frac{D-N_c}{2}; \frac{|\hat{\mathbf{q}}^{\perp}|^2 |\mathbf{k}^{\perp}(x_i)|^2}{(\hat{q} \cdot \tilde{\mathbf{k}}^{\parallel}(x_i))^2}\right)}{(\hat{q} \cdot \tilde{\mathbf{k}}^{\parallel}(x_i))^{N-N_c}} \quad (3.38)$$

where

$$\hat{q} \cdot \tilde{\mathbf{k}}^{\parallel}(x_i) \equiv -\tilde{\mathbf{k}}^0(x_i) + \hat{\mathbf{q}} \cdot \mathbf{k}^{\parallel}(x_i) \Big|_{\text{onshell cond.}} \quad (3.39)$$

Putting everything together, from (3.33) and (3.38) we get⁵

$$\begin{aligned} \text{div}(P^{N_c} R^{N-N_c}) \Big|_{D-N \geq 1} &= \frac{(-i)^{N-N_c}}{2^N (2\pi)^{D-N_c}} \text{Vol}(\mathbb{S}^{D-N_c-1}) \left[\frac{\Sigma_{cut}^{D-N_c-2}}{(\Sigma_{cut}^{space})^{D-N_c-1}} \right] \times \\ &\int_{\Delta^{N-N_c-1}} \left(\prod_{i=1}^{N-N_c} dx_i \right) \frac{{}_2F_1\left(\frac{N-N_c}{2}, \frac{N-N_c+1}{2}; \frac{D-N_c}{2}; \frac{|\hat{\mathbf{q}}^{\perp}|^2 |\mathbf{k}^{\perp}(x_i)|^2}{(\hat{q} \cdot \tilde{\mathbf{k}}^{\parallel}(x_i))^2}\right)}{(\hat{q} \cdot \tilde{\mathbf{k}}^{\parallel}(x_i))^{N-N_c}} \times \\ &\int |\mathbf{q}|^{D-N-2} d|\mathbf{q}| \left[1 + \mathcal{O}\left(\frac{1}{|\mathbf{q}|}\right) \right] \end{aligned} \quad (3.40)$$

We will now compute the explicit forms of the various $\tilde{\mathbf{k}}$ dependent factors in the integrand of the Feynman parameter integral above.

Since $\tilde{\mathbf{k}}^{\parallel}$ is the portion of $\tilde{\mathbf{k}}$ lying in the span of $\mathbf{k}_1, \mathbf{k}_2, \dots, \mathbf{k}_{N_c-1}$, let

$$\tilde{\mathbf{k}}^{\parallel} = \sum_{i=1}^{N_c-1} \alpha_i \mathbf{k}_i \quad (3.41)$$

for some $\{\alpha_i\}$.

Now consider the following system of $N_c - 1$ linear equations in α_i

$$\tilde{\mathbf{k}}^{\parallel} \cdot \mathbf{k}_j = \tilde{\mathbf{k}} \cdot \mathbf{k}_j = \sum_{i=1}^{N_c-1} \alpha_i (\mathbf{k}_i \cdot \mathbf{k}_j) \quad (3.42)$$

⁵Note this result has to be multiplied by 2 in the case where $D - N_c = 1$.

3 Non-local divergence at one-loop in open scalar field theories

Since k_i 's are linearly independent, the Gram matrix G made out of the k_i 's is invertible and thus we can invert the relations in (3.42) to obtain an expression for α_i

$$\alpha_i = \sum_{j=1}^{N_c-1} (G^{-1})_{ij}(\tilde{\mathbf{k}} \cdot \mathbf{k}_j) = \frac{1}{(\Sigma_{cut}^{space})^2} \sum_{j=1}^{N_c-1} (\text{adj } G)_{ij}(\tilde{\mathbf{k}} \cdot \mathbf{k}_j) = \frac{1}{(\Sigma_{cut}^{space})^2} \sum_{j=1}^{N_c-1} C_{ij}(\tilde{\mathbf{k}} \cdot \mathbf{k}_j) \quad (3.43)$$

where C_{ij} is the ij^{th} cofactor of the Gram matrix G . Note that in the last step we have used the fact that $C_{ij} = C_{ji}$. This is because G is a symmetric matrix.

Using (3.43) in (3.41), we obtain

$$\mathbf{k}^{\parallel} = \frac{1}{(\Sigma_{cut}^{space})^2} \sum_{i,j=1}^{N_c-1} C_{ij}(\mathbf{k} \cdot \mathbf{k}_j) \mathbf{k}_i = \frac{1}{(\Sigma_{cut}^{space})^2} \sum_{i=1}^{N_c-1} \begin{vmatrix} \mathbf{k}_1 \cdot \mathbf{k}_1 & \mathbf{k}_1 \cdot \mathbf{k}_2 & \cdots & \mathbf{k}_1 \cdot \mathbf{k}_{N_c-1} \\ \vdots & \vdots & \vdots & \vdots \\ \mathbf{k} \cdot \mathbf{k}_1 & \mathbf{k} \cdot \mathbf{k}_2 & \cdots & \mathbf{k} \cdot \mathbf{k}_{N_c-1} \\ \vdots & \vdots & \vdots & \vdots \\ \mathbf{k}_{N_c-1} \cdot \mathbf{k}_1 & \mathbf{k}_{N_c-1} \cdot \mathbf{k}_2 & \cdots & \mathbf{k}_{N_c-1} \cdot \mathbf{k}_{N_c-1} \end{vmatrix} \mathbf{k}_i \quad (3.44)$$

Note that for each i in the above sum, the terms $\mathbf{k} \cdot \mathbf{k}_j$ enter the i^{th} row of the corresponding determinant.

Taking dot product with \hat{q} on both sides of (3.44), we get

$$\hat{q} \cdot \mathbf{k}^{\parallel} = \frac{1}{(\Sigma_{cut}^{space})^2} \sum_{i=1}^{N_c-1} \begin{vmatrix} \mathbf{k}_1 \cdot \mathbf{k}_1 & \mathbf{k}_1 \cdot \mathbf{k}_2 & \cdots & \mathbf{k}_1 \cdot \mathbf{k}_{N_c-1} \\ \vdots & \vdots & \vdots & \vdots \\ \mathbf{k} \cdot \mathbf{k}_1 & \mathbf{k} \cdot \mathbf{k}_2 & \cdots & \mathbf{k} \cdot \mathbf{k}_{N_c-1} \\ \vdots & \vdots & \vdots & \vdots \\ \mathbf{k}_{N_c-1} \cdot \mathbf{k}_1 & \mathbf{k}_{N_c-1} \cdot \mathbf{k}_2 & \cdots & \mathbf{k}_{N_c-1} \cdot \mathbf{k}_{N_c-1} \end{vmatrix} k_i^0 \quad (3.45)$$

Then, using (3.45) we finally obtain the following compact expressions for $\hat{q} \cdot \tilde{\mathbf{k}}^{\parallel}$ and $\frac{|\hat{q}^{\perp}|^2 |\mathbf{k}^{\perp}|^2}{(\hat{q} \cdot \tilde{\mathbf{k}}^{\parallel})^2}$

$$\begin{aligned}
 \hat{q} \cdot \tilde{k}^{\parallel} &= -\tilde{k}^0 + \hat{q} \cdot \mathfrak{k}^{\parallel} = -\frac{\begin{vmatrix} \tilde{k}^0 & k_1^0 & \cdots & k_{N_c-1}^0 \\ \mathfrak{k} \cdot k_1 & k_1 \cdot k_1 & \cdots & k_{N_c-1} \cdot k_1 \\ \mathfrak{k} \cdot k_2 & k_1 \cdot k_2 & \cdots & k_{N_c-1} \cdot k_2 \\ \vdots & \vdots & \vdots & \vdots \\ \mathfrak{k} \cdot k_{N_c-1} & k_1 \cdot k_{N_c-1} & \cdots & k_{N_c-1} \cdot k_{N_c-1} \end{vmatrix}}{\begin{vmatrix} k_1 \cdot k_1 & k_1 \cdot k_2 & \cdots & k_1 \cdot k_{N_c-1} \\ k_2 \cdot k_1 & k_2 \cdot k_2 & \cdots & k_2 \cdot k_{N_c-1} \\ \vdots & \vdots & \vdots & \vdots \\ k_{N_c-1} \cdot k_1 & k_{N_c-1} \cdot k_2 & \cdots & k_{N_c-1} \cdot k_{N_c-1} \end{vmatrix}} \equiv -\frac{\tilde{\Sigma}_{cut}^0}{(\Sigma_{cut}^{space})^2} \\
 \frac{|\hat{q}^{\perp}|^2 |\mathfrak{k}^{\perp}|^2}{(\hat{q} \cdot \tilde{k}^{\parallel})^2} &= \frac{\begin{vmatrix} k_1 \cdot k_1 & k_1 \cdot k_2 & \cdots & k_1 \cdot k_{N_c-1} \\ k_2 \cdot k_1 & k_2 \cdot k_2 & \cdots & k_2 \cdot k_{N_c-1} \\ \vdots & \vdots & \vdots & \vdots \\ k_{N_c-1} \cdot k_1 & k_{N_c-1} \cdot k_2 & \cdots & k_{N_c-1} \cdot k_{N_c-1} \end{vmatrix} \begin{vmatrix} \mathfrak{k} \cdot \mathfrak{k} & \mathfrak{k} \cdot k_1 & \cdots & \mathfrak{k} \cdot k_{N_c-1} \\ k_1 \cdot \mathfrak{k} & k_1 \cdot k_1 & \cdots & k_1 \cdot k_{N_c-1} \\ \vdots & \vdots & \vdots & \vdots \\ k_{N_c-1} \cdot \mathfrak{k} & k_{N_c-1} \cdot k_1 & \cdots & k_{N_c-1} \cdot k_{N_c-1} \end{vmatrix}}{\begin{vmatrix} \tilde{k}^0 & k_1^0 & \cdots & k_{N_c-1}^0 \\ \mathfrak{k} \cdot k_1 & k_1 \cdot k_1 & \cdots & k_{N_c-1} \cdot k_1 \\ \mathfrak{k} \cdot k_2 & k_1 \cdot k_2 & \cdots & k_{N_c-1} \cdot k_2 \\ \vdots & \vdots & \vdots & \vdots \\ \mathfrak{k} \cdot k_{N_c-1} & k_1 \cdot k_{N_c-1} & \cdots & k_{N_c-1} \cdot k_{N_c-1} \end{vmatrix}^2} \equiv \frac{\Sigma_{cut}^2 (\tilde{\Sigma}_{cut}^{space})^2}{(\tilde{\Sigma}_{cut}^0)^2}
 \end{aligned} \tag{3.46}$$

Thus (3.40) can be re-written as follows⁶

$$\begin{aligned}
 \text{div}(P^{N_c} R^{N-N_c}) \Big|_{D-N \geq 1} &= \frac{i^{N-N_c}}{2^N (2\pi)^{D-N_c}} \text{Vol}(\mathbb{S}^{D-N_c-1}) \left[\frac{\Sigma_{cut}^{D-N_c-2}}{(\Sigma_{cut}^{space})^{D+N_c-2N-1}} \right] \times \\
 &\int_{\Delta^{N-N_c-1}} \left(\prod_{i=1}^{N-N_c} dx_i \right) \frac{{}_2F_1\left(\frac{N-N_c}{2}, \frac{N-N_c+1}{2}; \frac{D-N_c}{2}; \frac{\Sigma_{cut}^2 (\tilde{\Sigma}_{cut}^{space})^2}{(\tilde{\Sigma}_{cut}^0)^2}\right)}{\left(\tilde{\Sigma}_{cut}^0\right)^{N-N_c}} \times \\
 &\int |\mathbf{q}|^{D-N-2} d|\mathbf{q}| \left[1 + \mathcal{O}\left(\frac{1}{|\mathbf{q}|}\right) \right]
 \end{aligned} \tag{3.47}$$

The above expression looks fairly nasty! However, it is the most general expression for leading non-local divergence at one-loop level.

Special case: Non-local log divergence

⁶Note the result below has to be multiplied by 2 in the case where $D - N_c = 1$.

3 Non-local divergence at one-loop in open scalar field theories

Now, we specialize to the case of logarithmic divergence i.e. $D - N = 1$ where we will be able to glean complete information of the divergence structure. Then $D - N_c = N - N_c + 1$. The hypergeometric function sitting inside the integral over the $N - N_c - 1$ simplex reduces to just

$${}_2F_1\left(\frac{D - N_c - 1}{2}, \frac{D - N_c}{2}; \frac{D - N_c}{2}; \frac{\Sigma_{cut}^2 (\tilde{\Sigma}_{cut}^{space})^2}{(\tilde{\Sigma}_{cut}^0)^2}\right) = \frac{1}{\left(1 - \frac{\Sigma_{cut}^2 (\tilde{\Sigma}_{cut}^{space})^2}{(\tilde{\Sigma}_{cut}^0)^2}\right)^{\frac{D - N_c - 1}{2}}} \quad (3.48)$$

Now, we make a claim that the following non-trivial equation holds⁷:

$$(\tilde{\Sigma}_{cut}^0)^2 = \Sigma_{cut}^2 (\tilde{\Sigma}_{cut}^{space})^2 - (\Sigma_{cut}^{space})^2 \tilde{\Sigma}_{cut}^2 \quad (3.49)$$

Thus

$$1 - \frac{\Sigma_{cut}^2 (\tilde{\Sigma}_{cut}^{space})^2}{(\tilde{\Sigma}_{cut}^0)^2} = - \frac{(\Sigma_{cut}^{space})^2 \tilde{\Sigma}_{cut}^2}{(\tilde{\Sigma}_{cut}^0)^2} \quad (3.50)$$

and

$$\frac{1}{(\Sigma_{cut}^{space})^{-D + N_c + 1}} \times \frac{1}{(\tilde{\Sigma}_{cut}^0)^{D - N_c - 1}} \times \frac{1}{\left(1 - \frac{\Sigma_{cut}^2 (\tilde{\Sigma}_{cut}^{space})^2}{(\tilde{\Sigma}_{cut}^0)^2}\right)^{\frac{D - N_c - 1}{2}}} = \frac{\text{sgn}^{D - N_c - 1} (\tilde{\Sigma}_{cut}^0)}{(-\tilde{\Sigma}_{cut}^2)^{\frac{D - N_c - 1}{2}}} \quad (3.51)$$

Using the above expressions in (3.47), we get

$$\begin{aligned} \text{div}(P^{N_c} R^{D - N_c - 1}) &= \frac{i^{D - N_c - 1}}{2^{D - 1} (2\pi)^{D - N_c}} \text{Vol}(\mathbb{S}^{D - N_c - 1}) \Sigma_{cut}^{D - N_c - 2} \times \\ &\int_{\Delta^{D - N_c - 2}} \left(\prod_{i=1}^{D - N_c - 1} dx_i \right) \frac{\text{sgn}^{D - N_c - 1} (\tilde{\Sigma}_{cut}^0)}{(-\tilde{\Sigma}_{cut}^2)^{\frac{D - N_c - 1}{2}}} \log(\Lambda) \end{aligned} \quad (3.52)$$

⁷verified for large N_c on Mathematica, we skip an analytical proof at the moment

4 DISCUSSION OF RESULTS

In the last two chapters we find a number of new results about the divergence structure of cut diagrams at one loop in scalar field theories. Here we discuss about the implications and key ideas in some those results.

Through explicit computations we see that while the single cut C -type diagram C_{PRR} always diverges (see (2.11) of appendix), the double cut version of it (C_{PPR}) may be divergent (see (2.24)) or finite (see (2.32)) depending on whether the external momentum between the two cuts is space-like or time-like. Even in the case of the triple cut diagram, we are faced with two cases (see (2.41),(2.50)), although now the condition of divergence becomes a bit more complicated (depends on existence of a null plane formed by the external cut-cut momenta). In all the above cases, interestingly the divergences have a non-local structure, anything unlike ordinary Feynman diagrams in closed QFTs. This motivates us to ask the more general question: Under what circumstances do cut diagrams diverge at the one-loop level in a scalar field theory? Why are the divergences non-local? Is there a general structure to the form of the non-local divergence? These questions and more will be answered in this section.

Our discussion will be very general, meaning the arguments will apply to any arbitrary number of dimensions, external legs and cuts of one-loop cut diagrams in open scalar field theory. We will let D be the no of spacetime dimensions, N the no of external legs and N_c , the no of cuts such that $N_c \leq D$, N in the subsequent discussions.

4.1 SUPERFICIAL DEGREE OF DIVERGENCE OF CUT INTEGRALS

The superficial degree of divergence of a Feynman loop integral is defined to be the degree of the numerator(including the measure) minus the degree of the denominator. It is superficial because it gives a rough indication of the divergent behavior. In the case of integrals with off-shell propagators this definition works fine. For cut integrals, those we encounter in open QFTs, this definition fails to apply as delta functions do not admit Laurent expansions. We can however extend this notion after a careful examination of the way delta functions work inside cut integrals.

4 Discussion of results

We found in our explicit computations that the degree of divergence of cut integrals is $D - N - 1$ in contrast to $D - 2N$ (for cut-free integrals). This can be explained based on the following observation. A generic cut integral may be taken to be of the form (modulo constants)

$$\int d^D q \frac{\delta_+(q^2 + m_0^2) \prod_{i=1}^{N_c-1} \delta_+((q + k_i)^2 + m_i^2)}{\prod_{i=N_c}^{N-1} [(q + k_i)^2 + m_i^2 - i\epsilon]} \quad (4.1)$$

As we can see, the integral is over a bunch of delta functions and some ordinary Feynman propagators. If $N_c = D$, the delta functions will be able to eat up all the loop momentum variables, leaving behind no more integration to perform. This is a degenerate case and hence we assume $N_c < D$.

Coming back to the integral above, the first delta function in the numerator fixes the norm of the loop momentum and has the effect of linearizing all the initially quadratic dependencies (in loop momentum) in all the propagators (both onshell and offshell). The above integral (after integrating out q^0) looks like

$$\int \frac{d^{D-1} q}{2\sqrt{|\mathbf{q}|^2 + m_0^2}} \times \frac{\prod_{i=1}^{N_c-1} \delta_+(2q \cdot k_i + k_i^2 + m_i^2 - m_0^2)}{\prod_{i=N_c}^{N-1} [2q \cdot k_i + k_i^2 + m_i^2 - m_0^2 - i\epsilon]} \Big|_{q^0 = \sqrt{|\mathbf{q}|^2 + m_0^2}} \quad (4.2)$$

Now, in the UV sector (assuming the integral has support in the UV sector), the leading contribution to (4.2) comes from

$$\int \frac{d^{D-1} q}{2|\mathbf{q}|} \times \frac{\prod_{i=1}^{N_c-1} \delta(2q \cdot k_i)}{\prod_{i=N_c}^{N-1} (2q \cdot k_i)} \Big|_{q^0 = |\mathbf{q}|} \quad (4.3)$$

Each of the remaining delta functions can now be thought to be eating up a loop momentum angular coordinate, fixing some direction for \mathbf{q} and leaving behind a $\frac{1}{|\mathbf{q}|}$ factor (see (3.24) of appendix for details). This means we can consider both the onshell as well as offshell propagator as contributing -1 each in the overall degree of divergence, which naturally leads us to the previously stated expression for the UV degree of divergence i.e. $D - N - 1$.

4.2 NON-LOCALITY OF UV DIVERGENCES FROM NON-UNITARY CUTS

We find that one-loop Feynman diagrams with non-unitary cuts (i.e. made of P or M propagators but not both) in open scalar field theories, if UV divergent, are non-local. The non-locality stems from the presence of onshell (or cut) propagators where a ket state transforms to a bra state (or vice versa) with a matching energy flow direction. This kind of non-locality never arises at one loop in ordinary closed QFTs where Feynman diagrams are built from offshell propagators (except for the case of subgraph UV divergence; non-locality sometimes appear in higher-order loops where all loop momenta donot run to infinity together).

The answer to this apparent puzzle lies in the way an onshell propagator, being a Dirac-delta function, restricts the integration domain and further breaks spherical symmetry. Before discussing that, we first remind ourselves why closed QFTs admit only local UV divergences.

4.2.1 WHY ARE ONE-LOOP UV DIVERGENCES OF CLOSED QFTs LOCAL?

Let us first consider any UV-divergent one-loop diagram, of a closed scalar QFT, defined by imposing some regulator. The diagram can be made “more convergent” by differentiating wrt the external momenta. If q is the loop momentum and k is some linear combination of external momenta, then differentiating an offshell propagator wrt to k^μ gives

$$\frac{\partial}{\partial k^\mu} \left(\frac{-i}{(q+k)^2 + m^2 - i\epsilon} \right) = \frac{2i(q_\mu + k_\mu)}{[(q+k)^2 + m^2 - i\epsilon]^2} \sim \frac{1}{q^3} \text{ as } q \rightarrow \infty \quad (4.4)$$

We see from above that differentiating with respect to external momenta always increases the number of powers of q in the denominator. This is sufficient to conclude that if we differentiate the diagram sufficiently many times wrt the external momenta, the diagram will converge. Mathematically, if $I(k)$ is the integral corresponding to a particular Feynman diagram with external momenta k , then

$$\left(\frac{\partial}{\partial k} \right)^n I(k) = f(k) + \mathcal{O}\left(\frac{k}{\Lambda}\right) \quad (4.5)$$

where $f(k)$ is finite and independent of the cutoff regulator Λ . Integrating the above equation n times wrt the external momentum gives back our loop integral $I(k)$

$$I(k) = \tilde{f}(k) + P_n(k) + \mathcal{O}\left(\frac{k}{\Lambda}\right) \quad (4.6)$$

where $\tilde{f}(k)$ is finite and independent of Λ , and $P_n(k)$ is an n^{th} order polynomial in the external momentum that contains n constants of integration. We see that all of the terms that diverge as $\Lambda \rightarrow \infty$ must be in the constants of integration and hence must be polynomials in the external

momentum, or in other words, local. (As an aside, note that the finite part $\tilde{f}(k)$ contains all the non-trivial non-analytic structure of the diagram). The locality of these UV divergences is what allows us to cancel them via local counterterms in the Lagrangian and ultimately gives renormalized masses and couplings.

4.2.2 HOW IS DELTA FUNCTION RESPONSIBLE FOR UV DIVERGENCE NON-LOCALITY?

A delta function is naively thought to “localize” its argument inside integrals. So the fact it leads to non-local structure may at first come across as odd. But mind you, we are talking about non-locality in external momenta and not that of loop momentum (which it does localize), which qualifies us to ask a perfectly sensible question.

Is there any connection between localization of loop momentum via an onshell condition and non-locality (in external momenta) of the divergence?

The answer is yes! There is a very simple way to see this. It is based on the observation that onshell condition makes other propagators linear and breaks spherical symmetry.

If we look at (4.2), we find that the loop momenta are coupled to the external momenta as $q \cdot k_i$ terms inside the propagators. Now, assuming the integral has a support in the large momentum sector, we find that the k_i 's don't drop out in the UV limit due to the presence of the leading linear term. Further the “onshelled” propagators are always inversely proportional to the external momentum. This is the intuitive reason why we expect non-local structure for divergent cut diagrams. Note that this would not have happened if there were no delta function in which case the leading term of the propagators would have been quadratic in the UV sector.

4.3 MULTIPLE-CUT UV DIVERGENCE AND THE NULL PLANE OF CUT-CUT EXTERNAL MOMENTA

For single-cut one loop integrals, we found that positive degree of divergence was the sole factor behind UV divergence. However, just as we step up from single to double cut, we are faced with a “new” condition that needs to be satisfied first, before degree of divergence has anything to say. This new condition was whether the external momentum flowing between the two cuts is spacelike or timelike. Timelike cut-cut flow immediately shrunk the support of the integral to a bounded domain. For spacelike cut-cut flow, there was no such domain restriction, and it made sense to check the degree of divergence. Generalizing this to the case of multiple cuts lead us to the idea of a null plane worth of cut-cut external momentum flow. We will briefly outline the idea here.

Suppose the generic cut integral in (4.1) diverges in the UV sector. The leading UV piece of the integral will then look like the one in (4.3) provided the support of the integral itself is

4.3 Multiple-cut UV divergence and the null plane of cut-cut external momenta

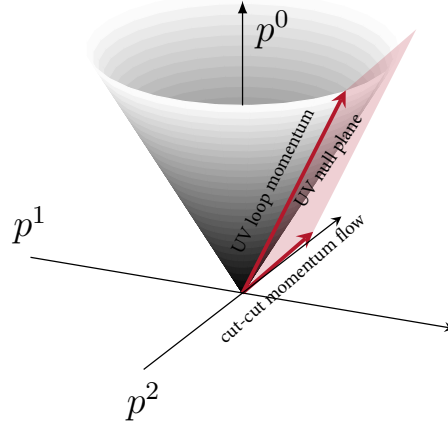


Figure 4.1: UV null plane of lightlike loop momentum and cut-cut momentum flow associated with a divergent B_{PP} diagram in 3 dimensions

unbounded. The support of the integral is determined by the delta functions. One of the delta functions ($\delta_+(q^2 + m_0^2)$) takes the loop momentum on the light cone in the UV sector. The other delta functions demand the “angular” constraints

$$q \cdot k_i = 0 \quad \forall i = 1, \dots, N_c - 1 \quad (4.7)$$

In other words, the support of the UV sector of the cut integral is on the light cone with $N_c - 1$ external cut-cut momentum flow orthogonal to it. This support is non-empty iff the external cut-cut momentum flow lie on a null plane.¹ Further, we want the cut-cut momentum flow to be linearly independent and span a $N_c - 1$ dimensional null plane, otherwise the onshell conditions will become dependent (result is zero in case of inconsistency, and delta function singularity in case of redundancy).

Thus we conclude that for cut integrals with $N_c \geq 2$, the UV divergence is always associated the existence of a null plane worth of external momentum flowing between cuts and we call this plane the UV null plane. It is this UV null plane from which the UV sector of the multiple-cut integral derives its support.

In figure (4.1) we have drawn a cartoon showing the UV null plane configuration for a divergent double cut diagram (B_{PP}) in three dimensions.

¹This can be seen very easily. If $|\mathbf{k}_i| = 0 \implies k_i^0 = 0$, i.e. k_i is zero. Since we k_i 's are chosen to be non-zero, this means that for a solution $\cos_i = \frac{k_i^0}{|\mathbf{k}_i|}$ and so k_i must be spacelike or null. Even though an external momenta flow could very well be along a null direction, we will not bother ourselves with the case where some external momentum flow is null (as it is a set of measure zero) and concentrate on the case where they are either space-like or time-like.

4.4 STRUCTURE OF NON-LOCAL DIVERGENCE ACROSS VARIOUS DIMENSIONS

In (3), we have done an exhaustive analysis of non-local divergences arising at one-loop in open scalar field theories. We will first provide a summary of the results obtained there.

In (4.1), we summarize the general form of the non-local log divergences appearing in cut diagrams in D spacetime dimensions. In D dimensions there are a total of $D - 1$ types of non-local log divergent diagrams viz. $PR^{D-2}, P^2R^{D-3}, P^3R^{D-4}, \dots, P^{D-1}$ all of which have $D - 1$ external legs. The extreme cases in this list are the single cut PR^{D-2} and the totally cut P^{D-1} .

It is worth noting that the divergence structure is not always Lorentz covariant because we are using cut-off regularization. We get Lorentz covariant answers only when $D - N_c - 1$ is a multiple of 2. For totally cut diagrams, the divergence is Lorentz covariant across all dimensions and for single cut diagrams, the divergence is Lorentz covariant only in even dimensions.

Diagram	Name	Divergence condition	Divergence structure ²
Single cut	PR^{D-2}	No condition	$\frac{i^{D-2} \text{Vol}(\mathbb{S}^{D-2})}{2^{D-1}(2\pi)^{D-1}} \int_{\Delta^{D-3}} \prod_{i=1}^{D-2} dx_i \frac{\text{sgn}^{D-2}(\tilde{k}^0)}{(-\tilde{k}^2)^{\frac{D-2}{2}}} \log(\Lambda)$
Totally cut	P^{D-1}	$\Sigma_{cut}^2 > 0, (\Sigma_{cut}^{space})^2 \neq 0$	$\frac{1}{2^{D-1}\pi} \frac{1}{\Sigma_{cut}} \log(\Lambda)$
Almost totally cut	$P^{D-2}R$	$\Sigma_{cut}^2 > 0, (\Sigma_{cut}^{space})^2 \neq 0$	$\frac{i}{2^D \pi} \frac{\text{sgn}(\tilde{\Sigma}_{cut}^0)}{\sqrt{-\tilde{\Sigma}_{cut}^2}} \log(\Lambda)$
Multiple cut	$P^{N_c} R^{D-N_c-1}$	$\Sigma_{cut}^2 > 0, (\Sigma_{cut}^{space})^2 \neq 0$	$\frac{i^{D-N_c-1}}{2^{D-1}(2\pi)^{D-N_c}} \text{Vol}(\mathbb{S}^{D-N_c-1}) \Sigma_{cut}^{D-N_c-2} \times \int_{\Delta^{D-N_c-2}} \prod_{i=1}^{D-N_c-1} dx_i \frac{\text{sgn}^{D-N_c-1}(\tilde{\Sigma}_{cut}^0)}{(-\tilde{\Sigma}_{cut}^2)^{\frac{D-N_c-1}{2}}} \log(\Lambda)$

Table 4.1: Non-local log divergences in one-loop diagrams with $D - 1$ external legs in D spacetime dimensions; Λ is a UV cutoff

EXAMPLES

The $D = 4$ case has already been done explicitly in (2.4). Here we use the formulae listed in (4.1) to write down all the non-local divergences in $D = 3, 4$ dimensions. At higher dimensions, the integrals grow in complexity and don't seem to admit any closed form expression.

- $D = 3$: There are two non-local log divergent bubble diagrams PR, P^2 .

²For the multiple cut case, the result given here should be multiplied by 2 if $N_c = D - 1$ which is nothing but the totally cut case

4.5 Diagram with atleast one unitary cut is always finite

Diagram	Divergence condition	Divergence structure
PR	None	$\frac{i}{8\pi} \frac{\text{sgn}(k^0)}{\sqrt{-k^2}} \log(\Lambda)$
P^2	$k^2 > 0$	$\frac{1}{4\pi} \frac{1}{\sqrt{k^2}} \log(\Lambda)$

Table 4.2: Non-local log divergences at one-loop in $D = 3$ spacetime dimensions; Λ is a UV cutoff

- $D = 4$: There are three non-local log divergent triangle (C-type) diagrams viz. PR^2, P^2R, P^3 .

Diagram	Divergence condition	Divergence structure
PR^2	None	$\frac{1}{16\pi^2} \frac{\tan^{-1}\left(\frac{\sqrt{\Sigma^2}}{k_1 \cdot k_2}\right)}{\sqrt{\Sigma^2}} \log(\Lambda)$
P^2R	$k_1^2 > 0$	$\frac{i}{16\pi} \frac{\text{sgn} \begin{pmatrix} k_2^0 & k_1^0 \\ k_2 \cdot k_1 & k_1 \cdot k_1 \end{pmatrix}}{\sqrt{-\Sigma^2}} \log(\Lambda)$
P^3	$\Sigma^2 > 0, (\Sigma^{space})^2 \neq 0$	$\frac{1}{8\pi} \frac{1}{\Sigma} \log(\Lambda)$

Table 4.3: Non-local log divergences at one-loop in $D = 3$ spacetime dimensions; Λ is a UV cutoff;
 $\Sigma^2 \equiv k_1^2 k_2^2 - (k_1 \cdot k_2)^2$, $(\Sigma^{space})^2 \equiv k_1^2 k_2^2 - (k_1 \cdot k_2)^2$

For the diagram P^2R in (4.3), the answer seems to be apparently different from the one calculated in (2.24). The mismatch is reconciled if we recall that the appendix computation was done in a special frame where $k_1^0 = 0$ (since k_1 is space-like). In the result above, if we substitute $k_1^0 = 0$, we find that the two results agree as expected.

4.5 DIAGRAM WITH ATLEAST ONE UNITARY CUT IS ALWAYS FINITE

Unitary cuts (or clean cuts) refer to a pair of P and M onshell propagators of a loop diagram. Presence of such a pair in any one-loop cut integral, renders it finite. This is because of the support coming from the step functions of the onshell propagators. Intuitively, the P and M

4 Discussion of results

propagators drive energy in the loop opposing directions and consequently renders the support of the integral bounded. The product of the step functions of the integral will be $\Theta(q^0 + \min(\{k_i\}_P))\Theta(-(q^0 + \max(\{k_i\}_M)))$. Now there are two cases:

- $\max(\{k_i\}_M) < \min(\{k_i\}_P)$: Then the integral is over the domain $-\min(\{k_i\}_P) < q^0 < -\max(\{k_i\}_M)$. Since $q^2 + m^2 = 0$ is one of the on-shell conditions, this means that ω_q integral is also over a finite domain. Hence the integral is finite.
- $\max(\{k_i\}_M) \geq \min(\{k_i\}_P)$: Then the support of q^0 becomes a measure zero set. Hence the integral is zero.

5 OUTLOOK AND FUTURE DIRECTIONS

We have presented a comprehensive case study of non-local divergences of one loop scalar cut integrals: their origin, structure and salient features in the bulk of this report. Not only are they mathematically rich and interesting, the fact that they are associated to physical processes in open systems means that this study and subsequent ones will usher a lot of new insights in the field of non-unitary open EFT. At the same time, it is almost self-explanatory that it is a fundamental roadblock in our goal towards a simple renormalizable open QFT. Non-local divergences cannot be absorbed into local counter terms of the Lagrangian. We hope that our study takes us a bit closer to understanding of the scheme that will eventually work to eliminate divergences and extract sensible expectation/correlation values measurable in experiments.

There are plenty of open questions that need to be answered hereafter. Apart from the obvious questions of finding renormalization schemes for the non-local divergences, there are many subtle questions like: How to derive EFT from an underlying microscopic theory? Are there open CFTs, open versions of Conformal blocks? Does non-local divergence appear in open versions of “most” QFTs? If so, what does that entail in terms of new physics? We think that a systematic study of the divergences, among many other things, can go a long way in understanding and hopefully solving some of these open problems.

BIBLIOGRAPHY

- [1] Avinash, C. Jana, R. Loganayagam, and A. Rudra. Renormalization in Open Quantum Field theory I: Scalar field theory. 2017. eprint: [arXiv:1704.08335](https://arxiv.org/abs/1704.08335).
- [2] H. P. Breuer and F. Petruccione. The theory of open quantum systems. Great Clarendon Street: Oxford University Press, 2002.
- [3] R. E. Cutkosky. “Singularities and discontinuities of Feynman amplitudes”. In: Journal of Mathematical Physics 1.5 (1960), pp. 429–433.
- [4] R. P. Feynman and F. Vernon Jr. “The theory of a general quantum system interacting with a linear dissipative system”. In: Annals of physics 281.1-2 (2000), pp. 547–607.
- [5] A. Kamenev. Field Theory of Non-Equilibrium Systems. Cambridge University Press, 2011. DOI: [10.1017/CB09781139003667](https://doi.org/10.1017/CB09781139003667).
- [6] L. V. Keldysh. “Diagram technique for nonequilibrium processes”. In: Zh. Eksp. Teor. Fiz. 47 (1964), p. 1018.
- [7] M. A. Luty. Physics 851 Lecture notes: Renormalization. URL: <https://www.physics.umd.edu/courses/Phys851/Luty/notes/renorm.pdf>. 2007.
- [8] J. Schwinger. “Brownian Motion of a Quantum Oscillator”. In: Journal of Mathematical Physics 2 (3 1961). DOI: [10.1063/1.1703727](https://doi.org/10.1063/1.1703727).
- [9] M. Veltman. Diagrammatica the Path to Feynman Diagrams. Cambridge University Press, 1994.